Nano Research

Open Access

Review Article

Advanced spectroscopic, microscopic, and compositional techniques in catalytic material characterization: Applications and progress

Rui Ren[1,2,§], Kai Guo[1,4,§], Yulan Gu[1,2], Guifen Li[1,2], Lirong Zhang[1,2], Yafu Wang[1,2], Qinnuan Zhang[1], Qin Wang[1,3] ✉, and Jiangwei Zhang[1,2,3,4,5] ✉

[1] *Inner Mongolia Key Laboratory of Low Carbon Catalysis, College of Energy Material and Chemistry, Inner Mongolia University, Hohhot 010021, China*
[2] *Inner Mongolia Advanced Research Institute, Hohhot 010021, China*
[3] *College of Chemistry and Chemical Engineering, Inner Mongolia University, Hohhot 010021, China*
[4] *Shanxi Meijin Energy Co., Ltd., Taiyuan 030000, China*
[5] *Key Laboratory of Advanced Energy Materials Chemistry, Nankai University, Tianjin 300071, China*
§ *Rui Ren and Kai Guo contributed equally to this work.*

Cite this article: *Nano Research*, **2026**, *19*, 94907814. https://doi.org/10.26599/NR.2025.94907814

ABSTRACT: Catalytic reactions play a key role in energy production, green chemistry, and chemical synthesis, and are the cornerstone for addressing global challenges such as environmental pollution and energy crisis. The design and performance optimization of efficient catalysts rely on a deep understanding of their structural characteristics, electronic states, and kinetic behaviors during reactions, and advanced characterization techniques provide key technical support. This review summarizes the applications, advantages, and limitations of spectroscopic techniques (X-ray absorption spectroscopy, nuclear magnetic resonance, Raman spectroscopy, infrared spectroscopy, and electron paramagnetic resonance), microscopic imaging techniques (transmission electron microscopy, scanning electron microscopy, and atomic force microscopy), and component analysis techniques (X-ray photoelectron spectroscopy, X-ray diffraction, and inductively coupled plasma mass spectrometry) in catalytic research. These techniques can provide multi-dimensional insights into the microstructure of catalysts, the properties of active sites, and their evolution during reactions, laying a solid foundation for elucidating catalytic mechanisms and optimizing catalyst performance. Although current characterization methods still face challenges in spatial resolution, compatibility with extreme reaction conditions, and data processing complexity, significant progress is expected through emerging strategies such as multi-technique integration and artificial intelligence-assisted analysis. This review aims to provide a reference for researchers in the field of catalysis and a forward-looking perspective for the development of characterization techniques.

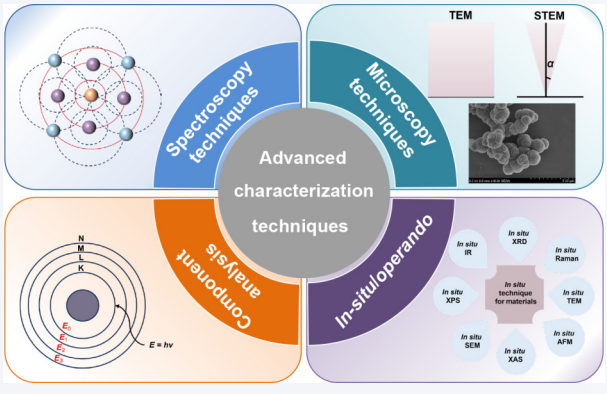

KEYWORDS: catalysis, spectroscopic techniques, microscopic imaging techniques, composition analysis, *in-situ* characterization

1 Introduction

Catalytic reactions are pivotal in tackling global challenges such as environmental pollution, energy shortages, and resource depletion [1]. As sustainable development goals gain prominence, catalysis has become central to advancing green chemistry and improving energy efficiency. Catalytic processes lower energy barriers, enhance selectivity, and reduce by-product formation, thereby minimizing environmental impact and promoting sustainable chemical production [2, 3].

The rational design and optimization of efficient catalysts hinge on a fundamental understanding of the structure–activity relationship [4–6]. This requires not only the accumulation of

Received: June 14, 2025; **Revised:** July 9, 2025
Accepted: July 17, 2025

✉Address correspondence to Qin Wang, qinwang@imu.edu.cn; Jiangwei Zhang, zjw11@tsinghua.org.cn, jwz@imu.edu.cn

experimental data but also the application of advanced characterization techniques that can probe catalyst properties across atomic, molecular, and macroscopic scales. These techniques enable the precise identification of active sites, monitoring of reaction intermediates, and elucidation of catalytic mechanisms, supporting the intelligent design of next-generation systems [7–9].

Advanced characterization methods—encompassing spectroscopy, microscopy, and compositional analysis—have thus become indispensable in catalysis research. They offer critical insights into structural, electronic, and chemical properties under both static and dynamic conditions, including *in situ* and *operando* environments. Despite recent advances, challenges remain in spatial/temporal resolution, operability under extreme conditions, and data interpretation complexity [10, 11].

To overcome these barriers, integrative strategies such as multi-technique coupling, real-time *operando* analysis, and artificial intelligence (AI)-assisted data processing are increasingly adopted. This review summarizes key characterization methods, highlights recent progress and limitations, and offers a forward-looking perspective on emerging technologies. By bridging existing gaps, these innovations are expected to drive deeper mechanistic insights and accelerate catalytic material discovery (Fig. 1).

2 Application of spectroscopic techniques in catalysis

Catalytic reactions are central to chemical transformations and are widely applied in fields such as energy production, green chemistry, and chemical synthesis. In the face of global challenges like environmental pollution, the energy crisis, and resource depletion, catalytic processes are playing an increasingly critical role in advancing green chemistry and promoting sustainable development. As a powerful tool for characterizing catalytic reactions, spectroscopic techniques offer valuable insights into the composition, structure, electronic state, and reaction kinetics of substances [12]. These insights are crucial for the design and optimization of catalysts and for the in-depth analysis of reaction mechanisms.

In recent years, the rapid development of surface science, catalytic reaction kinetics, and *in situ* spectroscopic methodologies has led to the widespread adoption of high-resolution, high-sensitivity spectroscopic techniques in catalytic research. Techniques such as X-ray absorption spectroscopy (XAS), nuclear magnetic resonance (NMR), Raman spectroscopy, infrared spectroscopy (IR), and electron paramagnetic resonance (EPR) have become instrumental in advancing our understanding of catalytic processes, particularly under *in situ* or *operando* conditions that mimic real reaction environments. These methods not only reveal the chemical state of catalyst surfaces and structural changes in reaction intermediates but also enable *in situ* real-time monitoring of reactant and product evolution during reactions [13, 14]. The integration of such *in situ* spectroscopic approaches allows researchers to capture dynamic changes in catalysts and intermediates under working conditions, bridging the gap between idealized models and practical catalytic systems. This makes them invaluable tools for gaining deeper insights into catalytic mechanisms and optimizing catalyst performance.

To better understand the specific features and complementarities of these spectroscopic techniques, Table 1 provides a comparison of the advantages, disadvantages, and inter-relationships of several key spectroscopic methods, including XAS, NMR, Raman, and IR. Notably, the ability to operate under *in situ* conditions is increasingly highlighted as a critical parameter in modern catalytic studies. This comparison can help researchers make more informed choices when applying these techniques in catalytic research. In this review, we will focus on the application of several spectroscopic techniques in catalysis. We will introduce the principles, characteristics, and *in situ* adaptability of these technologies in catalytic research to provide researchers in the field with a comprehensive reference for exploring and innovating catalytic reactions.

2.1 XAS

XAS is a powerful material characterization technique widely used in catalytic research, particularly for investigating catalyst surface and interface properties, elucidating reaction mechanisms, and monitoring dynamic changes during catalytic processes [15]. XAS

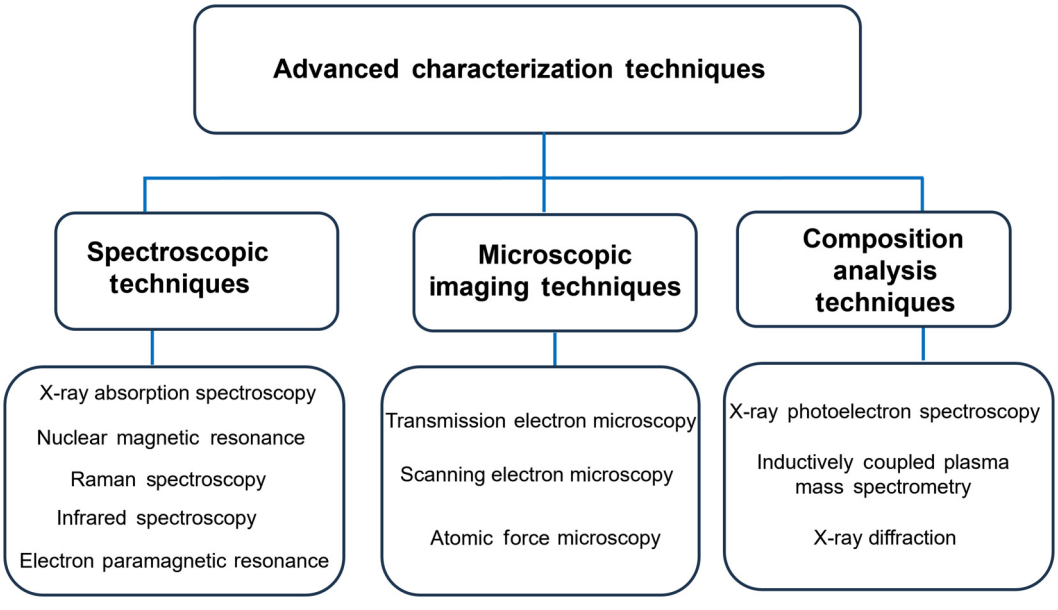

Figure 1 Classification of advanced characterization techniques presented in this article for catalysis research.

Table 1 Comparison of key features of selected characterization techniques in catalysis research

Technique	Advantages	Disadvantages	Inter-relationships
XAS	Provides local structural and electronic state information Applicable to amorphous systems Non-destructive	Sensitive to sample concentration	Complements EPR for metal centers Supplements NMR in analyzing metal environments
NMR	High resolution for detailed structure Probes molecular dynamics and interactions Quantitative analysis	Demands high sample purity Challenges with solids Expensive with high maintenance	Works with IR/Raman for vibrational/structural insights Complements XAS/EPR in metal systems
Raman	Non-destructive Minimal water interference Reveals bond and symmetry information	Weak signal and fluorescence interference Lower sensitivity at low concentrations Occasionally lower resolution than NMR/IR	Complements IR to cover the full vibrational spectrum Combined with NMR for comprehensive structural and local chemical data
IR	Fast measurements Rapid identification of functional groups Cost-effective	Interference from water Lower spatial resolution Limited to IR-active modes	Complements Raman for complete vibrational analysis Integrates with NMR/XAS for structural and functional evaluation
EPR	Highly sensitive to unpaired electrons Provides details on radicals and metal centers Controlled experimental conditions	Applicable only to paramagnetic samples Some experiments require low temperatures Limited structural detail	Complements XAS by detailing electronic states Combined with NMR and vibrational methods for a comprehensive analysis

provides detailed insights into the local structure, chemical environment, and electronic states of materials by analyzing the absorption characteristics of elements subjected to X-ray irradiation. Owing to its non-destructive nature, high selectivity, and ability to provide atomic-level structural information, XAS has become an indispensable tool in contemporary catalytic studies. XAS consists of two main components: X-ray absorption near edge structure (XANES) and extended X-ray absorption fine structure (EXAFS). XANES primarily provides insights into the valence state, coordination environment, and the relative position of the absorbing element concerning its surrounding atoms, making it particularly useful for studying redox changes in catalytic reactions [16]. Conversely, EXAFS offers detailed information about the local atomic structure, such as bond lengths and coordination numbers, and is particularly valuable for investigating structural changes at the surface and interface of catalysts. The XAS spectra typically include two regions: XANES, which provides information on the oxidation state and electronic structure (e.g., shifts in the absorption edge and variations in white-line intensity), and EXAFS, which reveals local coordination environments through the analysis of oscillation frequencies and amplitudes beyond the absorption edge.

The advent of *in situ* and *operando* XAS setups has significantly expanded their utility in catalysis research. By facilitating measurements under conditions closely resembling actual catalytic environments—such as high temperature, elevated pressure, and gas or liquid phases—*in situ* XAS enables real-time observation of dynamic structural and electronic transformations occurring within catalysts during operation. This capability is essential for identifying transient intermediates, monitoring the evolution of active sites, and establishing real-time correlations between structural motifs and catalytic performance [17].

Recent advancements in XAS technology have significantly contributed to catalytic research. By analyzing XAS spectra of catalysts under varying reaction conditions, researchers have uncovered crucial insights, including changes in active sites, interactions between metals and supports, and the structural evolution of reaction intermediates. These capabilities make XAS an essential tool for probing complex reaction mechanisms and optimizing catalyst performance.

For instance, Zhang et al. summarized the progress of nanocatalytic materials for small molecule conversion over the past five years [18]. Utilizing XAS, they identified the active components in the catalyst, monitored dynamic structural changes during reactions, and investigated the formation and evolution of stable reaction intermediates in transition metal single-atom catalysts, transition metal oxides, and metal polycrystals. Timoshenko et al. emphasized that XAS has become crucial in electrocatalysis, providing profound insights into the structural, chemical, and electronic transformations of catalysts under reaction conditions [19]. Yang et al. demonstrated the potential of synchrotron radiation XAS in catalytic research, particularly for revealing structural and electronic changes in complex catalysts (Fig. 2) [20]. Through *in situ* XAFS measurements, they observed the evolution of Zn/Co binuclear sites and their transformation during thermal cycling. XANES and EXAFS analysis indicated that, during heating, the Zn site exhibited a decrease in oxidation state, confirmed by a shift in the absorption edge and a reduction in coordination number, particularly at elevated temperatures (500–700 °C). This dynamic transformation contributed to higher catalytic activity in binuclear sites compared to monodispersed metal sites.

XANES and EXAFS techniques are invaluable for investigating the coordination environment of metal centers, variations in oxidation states, and the nature of metal–support interactions. For example, Wang et al. explored the electronic structure and atomic coordination of active sites in binuclear catalysts (Fig. 3), focusing on the influence of Fe and Co atom spatial configurations (stereo vs. planar) on catalytic performance in the oxygen evolution reaction (OER) [21]. Spectral analysis indicated that the planar Fe–Co binuclear site catalyst exhibited superior OER activity, which was attributed to enhanced metal–support interactions that optimized the electronic properties of Co atoms, thereby improving catalytic efficiency.

In conclusion, XAS, particularly XANES and EXAFS, plays an increasingly crucial role in catalytic research. By providing precise characterization of catalyst active sites and local structures, XAS offers new insights into catalytic mechanisms and delivers key data for the design and optimization of high-performance catalysts [22]. For a clearer understanding of the role of these techniques, the

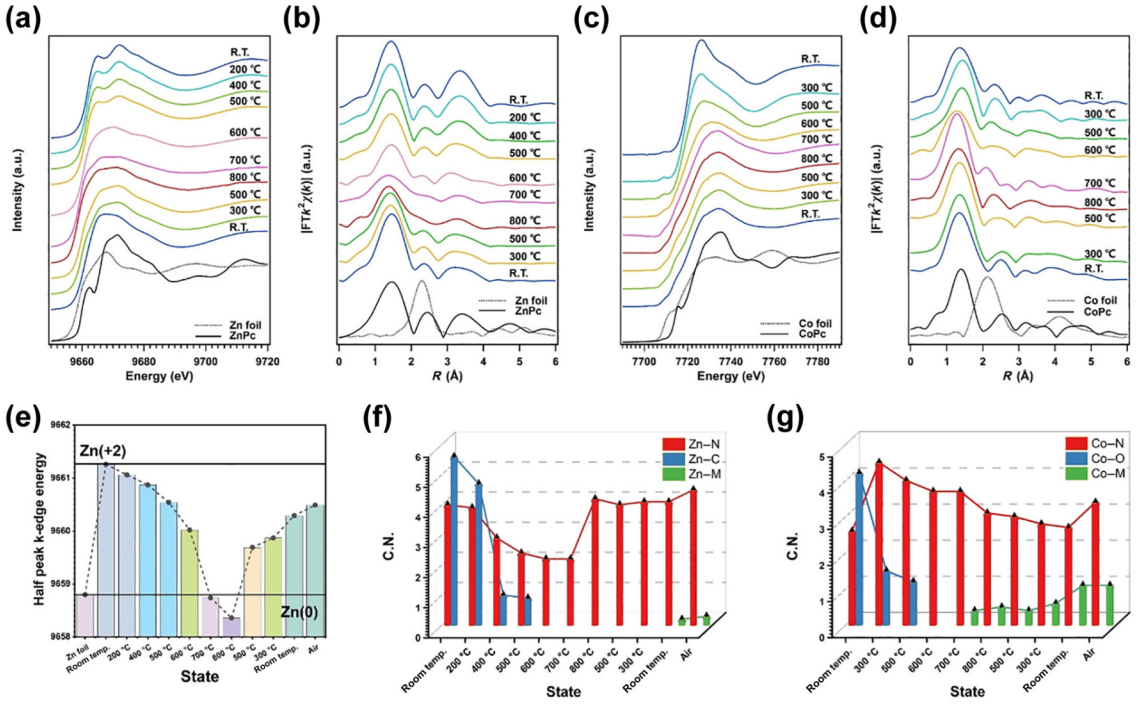

Figure 2 *In-situ* X-ray absorption spectroscopic analysis of Co-COF@MOF$_{800}$ as a function of temperature. (a) Zn k-edge XANES spectra of Co-COF@MOF at different temperatures and (b) k^2-weighted Fourier transform results. (c) *In-situ* Co k-edge XANES spectra of the catalyst at different temperatures and (d) k^2-weighted Fourier transform spectra of EXAFS. (e) Recording of the half-peak energy position of the Zn k-edge of the sample. (f) and (g) Summary of EXAFS fitting results of the Zn element and Co element. Reproduced with permission from Ref. [20], © Wiley-VCH GmbH 2023.

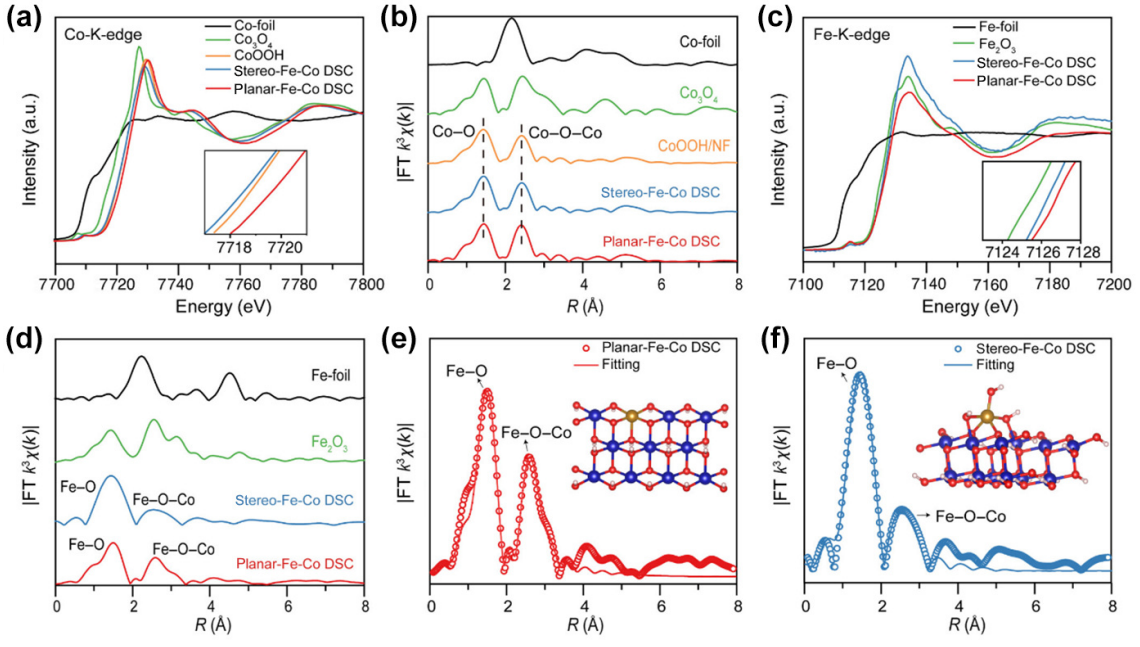

Figure 3 (a) The Co K-edge XANES spectra and (b) FT-EXAFS of cobalt foil, Co_3O_4, cobalt oxyhydroxide, stereo-Fe-Co dual-site catalyst (DSC), and planar-Fe-Co DSC. (c) The iron K-edge XANES spectra and (d) FT-EXAFS of iron foil, iron(III) oxide, stereo-Fe-Co DSC, and planar-Fe-Co DSC. Fe K-edge FT-EXAFS fitting curves of (e) planar-Fe-Co DSC and (f) stereo-Fe-Co DSC. Reproduced with permission from Ref. [21], © Zhang, T. Y. et al. 2024.

following section introduces the working principles and catalytic applications of NMR spectroscopy.

2.2 NMR

NMR is a powerful analytical technique with significant application value, especially in catalytic research. It plays a crucial role in analyzing the structure, reaction mechanisms, and dynamic processes of catalysts at the molecular level [23]. NMR technology operates based on the principles of nuclear spins. By applying an external magnetic field, it induces resonance in the nuclear spins of the sample, allowing for the extraction of detailed information about the atomic environment and molecular structure. Compared to other spectroscopic techniques, NMR provides high-resolution data on the internal structure, dynamics, electron density

distribution, and chemical environment of molecules. It is particularly valuable for analyzing metal coordination environments in organic molecules and catalysts [24].

In the field of catalysis, NMR can reveal essential information such as key intermediates, reaction pathways, and reaction rates, using precise parameters like chemical shifts, coupling constants, and relaxation times. For example, solid-state NMR is used to study the local structure of catalyst surfaces and metal centers. Particularly in complex multiphase catalytic systems, NMR can effectively distinguish different types of reactants and products, offering critical support for catalyst design and an in-depth analysis of reaction mechanisms [25, 26]. Additionally, the high sensitivity and resolution of NMR make it indispensable for studying tiny structural changes, catalyst deactivation mechanisms, and the evolution of catalytic reaction intermediates during the catalytic process. With technological advancements, the application of NMR has expanded beyond traditional liquid-phase catalytic systems to more complex solid-phase catalytic systems, broadening its application prospects for structural optimization and a deeper understanding of catalytic reaction mechanisms.

For example, Michiel et al. developed an atomically dispersed low-load Ru catalyst supported on β-zeolite by combining isomerization with the Diels–Alder cycloaddition reaction (Fig. 4(a)) [27]. The catalyst produced trans, trans-hexadienedioic acid in ethanol with a total conversion rate and selectivity above 95%, successfully overcoming the isomer equilibrium. The isomerization mechanism was confirmed through isotope-labeled NMR, which demonstrated the formation of Ru hydride intermediates from alcohol solvents. In addition, the regulation of active centers in zeolites is closely related to the design of their framework structures, providing new insights into this relationship for Mo-doped zeolites. Sun et al. reported a new catalytically active center with an unsaturated tricoordinated cobalt unit ((≡Si–O)CoO(O–Mo)) anchored within a Mo-doped silica molecular sieve [28]. Using ^{29}Si solid-state magic angle spinning nuclear magnetic resonance (MAS NMR) and ^{31}P MAS NMR, they showed that Mo doping significantly reduced silanol defects in the molecular sieve, forming a silanol-free Mo-S-1 molecular sieve framework. Additionally, ^{31}P MAS NMR analysis revealed the interaction between trimethylphosphine oxide (TMPO) and Mo atoms, confirming the isomorphic substitution effect of Mo in the framework. These NMR characterization results not only clarify the active center's structural regulation mechanism but also provide theoretical support for the design of molecular sieve catalysts.

Solid-state NMR technology is an important tool for studying zeolite molecular sieves, and can provide atomic-level structural and dynamic information [29–31]. Deng et al. systematically summarized the key strategies of solid-state NMR technology in the characterization of molecular sieve framework structure (Fig. 4(b)) [29]. With the continuous development of high-field spectrometers and hyperpolarization signal enhancement technology, the sensitivity and resolution of solid-state NMR have been significantly improved. For common atoms such as Si and Al in the molecular sieve framework, atomic positioning information can be obtained through chemical shift. For example, one-dimensional and two-dimensional NMR technology can analyze the type, content, and distribution information of acidic sites, and quantitatively reflect the acidic strength through alkaline probe molecules. In addition, NMR technology can reveal the nature of molecular interactions by characterizing specific atomic correlations between the active sites of molecular sieves and guest molecules, as well as between different guest molecules. For instance, the application of one-dimensional and two-dimensional ^{13}C–^{27}Al and ^{13}C–^{13}C solid-state NMR techniques has been instrumental in characterizing supramolecular active centers within the confined pores of molecular sieves. These techniques also help in studying "cation–π interactions" between guest molecules, offering new insights into the catalytic mechanisms of molecular sieves [32].

Although NMR spectroscopy offers unique advantages in achieving atomic-level resolution for catalysis research, its widespread application is still hindered by several limitations [33–35]. Foremost among these is its inherently low sensitivity: detecting nuclei with low natural abundance or low gyromagnetic ratios often requires isotope enrichment or hyperpolarization techniques to enhance signal intensity [36–38]. Moreover, the detection of trace species frequently necessitates prolonged signal accumulation, particularly in solid-state NMR, where the acquisition of high-resolution spectra can take several hours to even days [39].

In addition to sensitivity constraints, the high cost of instrumentation and stringent sample preparation requirements further limit the accessibility and universality of NMR [40]. Solid-state NMR faces additional challenges, including peak broadening caused by dipolar couplings and chemical shift anisotropy, as well as difficulties in quantitative analysis due to variations in cross-polarization efficiency and nuclear relaxation times. Furthermore, the presence of paramagnetic species such as Fe^{3+} can interfere with signal acquisition (quenching of ^{1}H NMR signals), making it challenging to characterize transition metal-based catalytic systems [41].

Despite these challenges, NMR spectroscopy remains an indispensable tool in catalysis research, offering non-destructive,

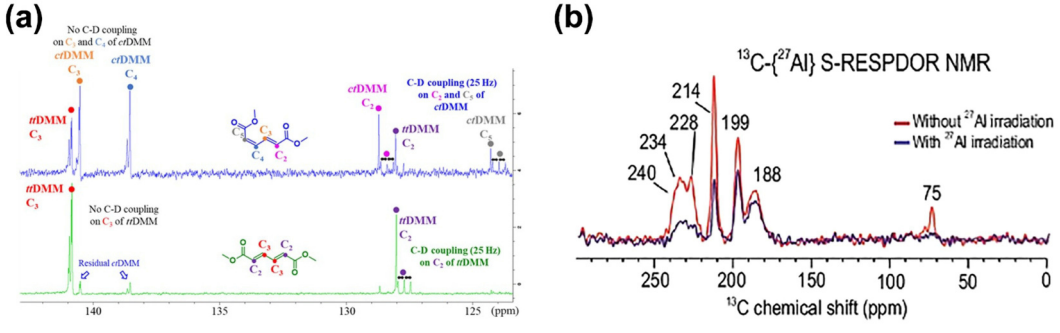

Figure 4 (a) ^{13}C-NMR spectra of the isomerization reaction of *ct*-dimethyl muconate (*ct*DMM) with deuterated methanol. Reproduced with permission from Ref. [27], © American Chemical Society 2017. (b) ^{13}C–^{27}Al NMR spectra of 2–^{13}C-acetone loaded on dealuminated HY zeolite. Reproduced with permission from Ref. [29], © Wang, W. Y. et al. 2022.

high-resolution, and multidimensional dynamic insights at the atomic scale. Recent developments in multi-technique integration—such as coupling with XAS and electron microscopy—are progressively enhancing NMR's sensitivity, temporal resolution, and compatibility with complex reaction environments. In the future, NMR is expected to play a pivotal role in elucidating dynamic mechanisms in intricate catalytic systems, including single-atom catalysis and multiphase interfacial reactions. While NMR spectroscopy provides valuable insights into the local chemical environment and molecular dynamics of catalytic systems, it is often complemented by vibrational techniques such as Raman spectroscopy, which offer surface-sensitive and structural information on active species and reaction intermediates. The following section introduces the fundamental principles of Raman spectroscopy and highlights its representative applications in catalytic reaction studies.

2.3 Raman spectroscopy

Raman spectroscopy is a non-destructive, label-free analytical technique that is widely applied across disciplines including chemistry, physics, and materials science [42]. Since its discovery in 1928 by Indian physicist C. V. Raman, it has served as a fundamental tool in characterizing molecular structures, investigating vibrational and rotational modes, and monitoring variations in the chemical environment. By analyzing shifts in the frequency of scattered light, researchers can extract detailed information about the internal structure, composition, chemical bonding, and molecular interactions of substances [43].

The emergence of *in situ* Raman spectroscopy has further enhanced its transformative impact in catalysis [44]. Through integration with specialized reaction cells and controlled environments, *in situ* Raman facilitates direct observation of catalytic processes under realistic operational conditions, such as electrochemical polarization, gas flow, or thermal activation. This approach captures transient intermediates, surface adsorbates, and structural rearrangements that elude conventional characterization, thereby providing molecular-level insights into dynamic reaction pathways.

In recent decades, progress in Raman spectroscopy has substantially broadened its capabilities, enabling high-resolution analysis, the development of surface-enhanced Raman spectroscopy (SERS), and integration with other analytical techniques [45]. Notably, as a highly efficient and non-destructive vibrational spectroscopic technique, Raman spectroscopy offers distinct advantages in the structural characterization of catalytic materials, tracking reaction intermediates, and *in situ* monitoring of dynamic processes [46]. Its high compatibility with aqueous environments, broad adaptability to various sample morphologies, ability to track temporal-spatial evolution of species, and synergy with surface enhancement techniques have established it as a critical tool for elucidating complex catalytic mechanisms. Particularly in catalysis research, *in situ* Raman spectroscopy has garnered significant attention due to its capability to monitor the dynamic evolution of catalyst surface structures under working conditions [47]. A representative example that exemplifies the analytical power of *in situ* Raman spectroscopy is presented in the study by Pan et al. [48]. The researchers utilized copper foam (CF) as a support substrate and prepared the R-CoCu@CF catalyst via *in situ* electrochemical deposition (Fig. 5(a)). Raman spectroscopy was employed to investigate the structural changes of the catalysts (Figs. 5(b)–5(f)). For CoCu@CF, the characteristic peaks of Cu_2O and $Cu(OH)_2$ gradually diminished and eventually disappeared at 0.2 V (Fig. 5(c)), signaling their reduction to metallic Cu. For Co@CF, the applied potential induced a phase transition from α-$Co(OH)_2$ to β-$Co(OH)_2$, accompanied by a blue shift in the vibrational modes of cobalt hydroxide and alterations in the Co–O coordination environment. In CoCu@CF, the peaks corresponding to $Cu(OH)_2$ and Cu_2O rapidly disappeared at −0.3 V, signifying complete reduction to metallic Cu, while the vibrational peaks of β-$Co(OH)_2$ appeared at 450 and 510 cm^{-1}. These potential- and time-dependent spectral evolutions, captured through *in situ* Raman monitoring, yielded critical insights into the dynamic surface structure of Cu- and Co-based catalysts. Such observations further confirmed catalyst phase transitions and stability, demonstrating how *in situ* Raman bridges the gap between electrochemical stimuli and real-time structural responses—providing valuable insights into catalytic mechanism studies. Moreover, Raman spectroscopy demonstrates significant complementarity and synergy in the characterization of complex catalytic systems when integrated with multimodal techniques. In the work of Hess, density functional theory (DFT) calculations were utilized to aid in the assignment of Raman peaks, enabling precise correlation between vibrational modes and surface chemical bonding states. Coupling Raman spectroscopy with XAS and IR enabled the development of multidimensional structure–activity relationship models for catalysts [46]. Zhu et al. further utilized *in situ* Raman spectroscopy in conjunction with XANES to comprehensively investigate the reaction mechanism of sulfur cathodes (S_8) in all-solid-state lithium-sulfur batteries [49].

However, numerous challenges continue to impede the practical applications of Raman spectroscopy, including fluorescence interference, weak signal intensity, limited spatial representativeness, and difficulties in characterization under high-temperature or high-pressure conditions. Therefore, future efforts should focus on improving signal sensitivity, suppressing background interference, and expanding *in situ* testing capabilities under extreme conditions, to further augment its potential and value in energy catalysis research [50]. Raman spectroscopy and IR spectroscopy are two complementary vibrational spectroscopic techniques widely employed in catalysis research to probe molecular structures, reaction intermediates, and surface species. Both techniques provide fingerprint information based on the vibrational modes of chemical bonds, enabling the identification of adsorbed reactants and products as well as mechanistic pathways. Raman spectroscopy, relying on inelastic scattering of monochromatic light, is particularly suitable for studying symmetric, non-polar bonds, and can be conducted through transparent windows under *operando* conditions. IR spectroscopy, on the other hand, is sensitive to dipole moment changes and is highly effective in detecting polar functional groups.

2.4 IR spectroscopy

Both infrared spectroscopy and Raman spectroscopy are based on molecular vibrations and are frequently employed in tandem within catalysis research to yield complementary insights into molecular vibrational characteristics [51–53]. Although both techniques reveal vibrational modes, they operate via distinct response mechanisms, granting each method unique advantages and optimal application domains. To further illustrate the complementarity of infrared and Raman spectroscopy in catalysis research and delineate their differences across various aspects, Table 2 provides a detailed comparison of their respective attributes. This comparison not only enhances researchers' understanding of the distinct characteristics

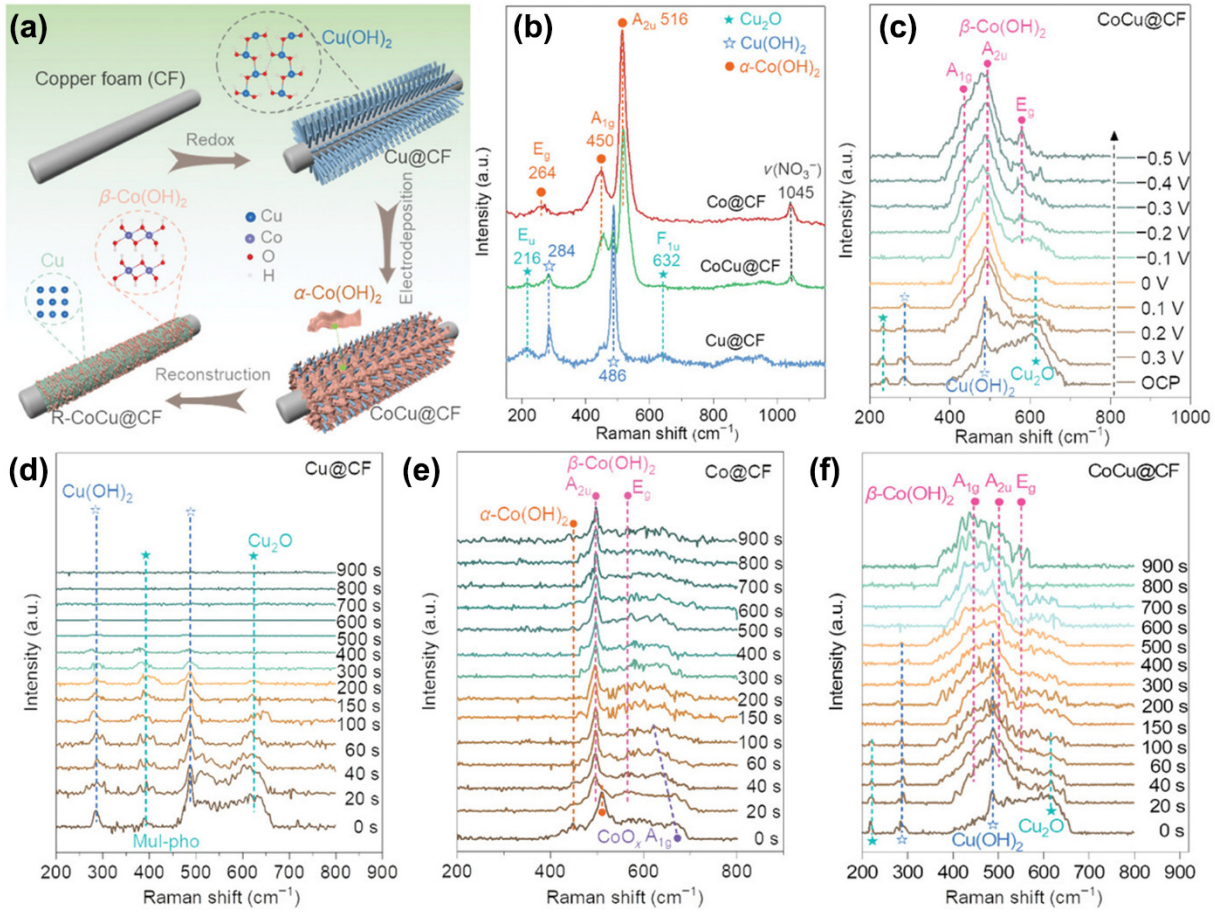

Figure 5 (a) Schematic diagram of R-CoCu@CF. (b) *Out-of-situ* Raman spectra of different samples. (c) Potential-dependent *in situ* Raman spectroscopy at CoCu@CF. *In situ* Raman spectra of (d) Cu@CF, (e) Co@CF, and (f) CoCu@CF at −0.3 V vs. RHE. Reproduced with permission from Ref. [48], © Qiao, L. L. et al. 2024.

Table 2 Comparing the similarities and differences between infrared spectroscopy and Raman spectroscopy

Comparison items	Infrared spectroscopy	Raman spectroscopy
Principle	Interaction between infrared light and molecular vibrations Molecules absorb specific infrared frequencies when vibrations cause changes in dipole moment	Interaction between monochromatic light and molecular vibrations via inelastic (Raman) scattering Raman activity arises from a change in molecular polarizability
Suitable samples	Polar molecules (containing polar bonds)	Non-polar and symmetric molecules It can detect symmetric vibration modes that are difficult to detect by IR
Detected signals	Absorption signals (absorption of infrared light by molecules)	Scattering signals (detecting Raman-scattered light)
Sample requirements	Samples usually need to be prepared in appropriate forms	Directly detect solid, liquid, and gas samples
Spectral features	Absorption peak intensity is related to the change in dipole moment of molecules Larger dipole-moment changes result in stronger absorption peaks	Peak intensity is related to the change in polarizability of molecules Larger polarizability changes lead to stronger Raman peaks
Similarities	Both are used to analyze molecular vibration and rotation information for determining molecular structure and chemical bond situations. Both belong to spectroscopic analysis techniques and are widely applied in chemistry, materials science, biological science, etc.	

of each method but also guides the selection of appropriate spectroscopic techniques for specific catalytic investigations. Building upon this comparative understanding, it is essential to further explore the unique role and strengths of infrared spectroscopy in catalysis research. Infrared spectroscopy is an indispensable characterization tool in catalysis research, particularly for probing active sites on catalyst surfaces, identifying reaction intermediates, and elucidating reaction mechanisms [54]. By analyzing the vibrational modes of substances involved in the catalytic process, infrared spectroscopy provides valuable information regarding molecular structure, chemical bonding, and surface interactions. In catalytic reactions, especially those involving gas–solid or liquid–solid interfaces, infrared spectroscopy can track real-time interactions at the catalyst–reactant interface, revealing changes in catalyst reactivity and the dynamic evolution of surface properties [55]. As an advanced characterization technique, infrared

spectroscopy plays a vital role in advancing the understanding of catalytic mechanisms and informing the rational design of catalysts. A recent study employed both *in situ* attenuated total reflection surface-enhanced infrared absorption spectroscopy (ATR-SEIRAS) and Raman spectroscopy to investigate CO electroreduction to n-propanol over Sn–Cu atomic alloy catalysts [56]. ATR-SEIRAS revealed red-shifted CH_2O C=O vibrations and a new peak, indicating stable bridge-bound CH_2O species on Sn–Cu dual sites, which facilitate C_1–C_2 coupling. Complementary Raman spectra showed enhanced low-frequency bridge CO adsorption without significantly altering Cu–CO behavior, suggesting selective promotion of coupling pathways. This combined approach elucidated the role of intermediate stabilization in boosting n-propanol selectivity. Another representative example employed *in situ* Fourier transform infrared (FTIR) spectroscopy and Raman spectroscopy to investigate the oxygen reduction reaction (ORR) mechanism on PtPdFeCoNiMo high-entropy alloys (HEMs) [57]. *In situ* FTIR spectra revealed characteristic peaks at 1204 cm^{-1} (OOH), 1426 cm^{-1} (O_2), 1636 cm^{-1} (adsorbed H_2O), and 3532 cm^{-1} (OH), with OOH signal intensity increasing with potential. Complementary Raman analysis showed a surface-adsorbed O species peak at 1121 cm^{-1}, whose intensity decreased with increasing voltage, indicating reduced surface oxygen coverage and enhanced ORR activity. Chen et al. designed and synthesized covalent organic polymers based on iron phthalocyanine as electrocatalysts to investigate the structure–performance relationship of ORR [54]. To further confirm the structure of the prepared catalyst, FTIR spectroscopy was employed. The FTIR spectra showed a stretching vibration peak around 1120 cm^{-1}, which was attributed to the coordination bond between the central Fe atom and the N atom in the phthalocyanine ring. A peak at approximately 900 cm^{-1} corresponded to the vibration of the metal–ligand bond. Additionally, the peak around 736 cm^{-1} represented the characteristic vibration of the main chain, while the peaks at about 1445 and 1586 cm^{-1} were associated with the stretching vibrations of the C=C and C=N bonds, respectively, that connect the structural units. The presence of these characteristic peaks confirmed the successful synthesis of the target catalysts and provided strong evidence for their molecular structure. These infrared spectral data highlight the crucial role of FTIR in catalyst characterization, as it effectively reveals the vibrational features of various chemical bonds in the catalyst and aids in understanding the relationship between its structure and catalytic performance. Similarly, Ma et al. synthesized Rh-supported catalysts containing both isolated Rh sites and ensemble Rh cluster sites (Rh_{1+n}/ND@G, where n represents the number of clusters) using a deposition–precipitation method. These catalysts were then evaluated for their performance in the cyclohexanol dehydrogenation reaction. *In situ* FTIR spectroscopy was employed to investigate the reaction behavior of cyclohexanol on the different catalysts (Fig. 6). Although surface species could not be directly observed, significant changes in the infrared bands associated with

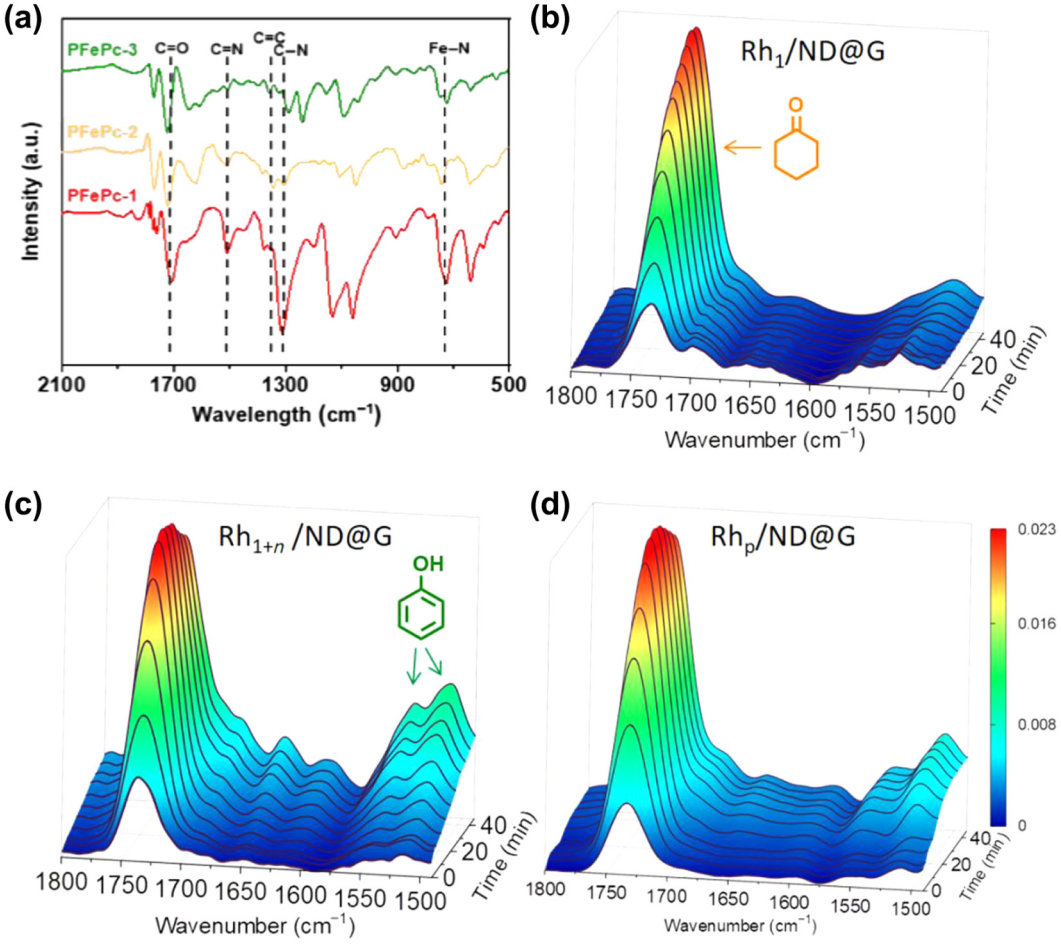

Figure 6 (a) FTIR spectra of three catalysts. Reproduced with permission from Ref. [54], © Wiley-VCH GmbH 2025. *In situ* infrared spectra of (b) Rh_1/ND@G, (c) Rh_{1+n}/ND@G, and (d) Rh_p/ND@G for cyclohexanol dehydrogenation. Reproduced with permission from Ref. [58], © American Chemical Society 2022.

the reaction products, cyclohexanone and phenol, were observed over time. Notably, at 240 °C, the ν(C–O) bond at 1735 cm^{-1} disappeared after the introduction of cyclohexanol, indicating that the formation of cyclohexanone was closely linked to the activity of the Rh catalytic sites. Despite the low rhodium loading in the Rh/ND@G catalyst, a considerable amount of cyclohexanone was produced, suggesting that its Rh sites exhibited a high reaction rate for cyclohexanol conversion. As the reaction progressed, the intensity of the ν(C–O) bond on the Rh_1/ND@G catalyst gradually stabilized, with no additional products detected. In contrast, on the Rh_{1+n}/ND@G and Rh_p/ND@G catalysts, the signals at 1540 and 1512 cm^{-1} increased, and the intensity of the ν(C=O) bond decreased, indicating that these catalysts could further convert cyclohexanone into phenol. These *in situ* FTIR data provide valuable insight into the dynamic evolution of reactants and products on the catalyst surface, offering a solid experimental basis for understanding the role of different catalytic sites in the reaction mechanism [58].

In situ Fourier transform infrared spectroscopy has emerged as a powerful technique for unveiling the dynamic processes of electrocatalytic reactions. It enables real-time tracking of intermediate species on the catalyst surface and provides direct molecular-level evidence for in-depth mechanistic investigations. For example, in the electrocatalytic nitrate reduction reaction (NO_3^-RR), *in situ* FTIR was employed to successfully monitor the stepwise transformation of NO_3^- on a $Cu_5/Mo_{0.6}$-WO_3 catalyst surface. As the applied potential was gradually scanned in the negative direction to −0.7 V reversible hydrogen electrode (RHE), the characteristic absorption bands of NO_3^- (1356 and 1382 cm^{-1}) progressively diminished. Concurrently, signals corresponding to intermediate species such as $*NO_2$ (1230 and 1590 cm^{-1}), *NO, and the hydrogenated intermediate NH_2OH (1160 and 1285 cm^{-1}) appeared sequentially. These observations clearly delineated a cascade reaction pathway: $NO_3^- \rightarrow *NO_2 \rightarrow NO \rightarrow NH_2OH \rightarrow NH_3$. This study not only demonstrates the unique advantages of *in situ* FTIR in unraveling complex electrocatalytic pathways but also provides critical scientific insight for the rational design of high-performance tandem catalyst systems [59].

2.5 EPR

EPR is a powerful spectroscopic technique widely employed in catalytic research, particularly for characterizing metal catalysts and analyzing reaction mechanisms [60–62]. EPR detects substances with unpaired electrons, offering valuable insights into the electronic structure, coordination environment, and reaction intermediates at the metal center. Due to its high sensitivity and ability to operate under various temperature and pressure conditions, EPR is instrumental in investigating catalyst active sites, electron transfer mechanisms during reactions, and the stability and deactivation processes of catalysts [63]. Recent advancements in EPR technology, particularly with the development of high-frequency EPR and electron spin resonance (ESR), have enabled the precise capture and analysis of complex electronic states and dynamic processes in catalytic systems. Thus, EPR not only provides a critical experimental foundation for designing and optimizing catalytic materials but also contributes to the deeper understanding of catalytic reaction mechanisms. Hu et al. developed a hierarchical W-CCNs catalyst with functional separation characteristics to achieve the synergistic effect of multiple defect active sites in electrocatalytic reduction of nitrate reaction (eNO_3^-RR). In order to detect the paramagnetic center in the sample, EPR spectroscopy was performed [64]. Both W-CCN and W-CCNs-1100 showed obvious EPR signals, g = 2.002 (Fig. 7(a)), which originated from free electrons caused by topological defects. The difference in peak intensity may be related to the higher defect density in W-CCN, while no EPR signal was observed in p-CNT due to the lack of topological defects. Song et al. developed a $CoFe_2O_4$@CoBDC catalyst with a core–shell structure (Fig. 7(b)) [65]. The structural and electronic state changes of the catalyst under magnetic field regulation were analyzed by EPR. The results showed that the generation of oxygen vacancies (VO) increased, and the proportion of divalent cobalt increased significantly.

Unlike EPR, ESR analysis focuses on the interaction between the magnetic moment generated by the electron spin angular momentum and the external magnetic field. Feng et al. prepared NiS/$NiFe_2O_4$ composites by inducing a phase reconstruction in defective S-doped $NiFe_2O_4$ using a plasma-induced method. The ESR spectrum shown in Fig. 7(c) reveals important insights into the defect characteristics of the material. The ESR signal at g = 2.003 corresponds to unpaired electrons trapped by oxygen vacancies in the sample. A subtle peak is observed in $NiFe_2O_4$, while S-$NiFe_2O_4$ exhibits a stronger ESR signal, indicating that sulfur (S) atoms induce a significant increase in VO in $NiFe_2O_4$ [66].

The hollow cobalt phosphide nanosphere electrocatalyst (CoP-CNS), reported by Shao's research team, demonstrated excellent catalytic performance in the nitrate reduction reaction for ammonia production. To elucidate its reaction mechanism, the researchers systematically investigated the existence and role of the key intermediate, hydrogen adsorption species (H_{ads}), using ESR technology. The experiment employed 5,5-dimethyl-1-pyrrolidine-N-oxide (DMPO) as a free radical scavenger, and *in situ* analysis was conducted on the CoP-CNS catalytic system in a 1.0 M OH^- electrolyte containing varying concentrations of NO_3^- (0–1.0 M) (Fig. 7(d)). The results revealed that under pure alkaline electrolyte conditions (without NO_3^-), a typical 9-fold splitting peak appeared in the ESR spectrum, corresponding to the characteristic signal of DMPO-H spin adducts, confirming the generation of H_{ads} during water decomposition. Notably, as the NO_3^- concentration increased from 0.1 M to 1.0 M, the intensity of the DMPO-H signal decreased in a concentration-dependent manner, and at a NO_3^- concentration of 1.0 M, the characteristic signal completely disappeared. This observation strongly supports the idea that the two key steps of the nitrate reduction reaction—deoxygenation and hydrogenation consume the H_{ads} intermediates generated from electrocatalytic water decomposition, thus revealing the dual role of H_{ads} in this catalytic system [67].

In summary, EPR spectroscopy serves as a powerful and irreplaceable technique for elucidating the local electronic environment, identifying paramagnetic intermediates, and probing reaction mechanisms in catalytic systems [68]. Its ability to detect unpaired electrons provides unique insights into radical species and transition metal centers that are often elusive to other spectroscopic methods. Although current limitations—such as restricted applicability, demanding experimental conditions, and complex spectral analysis—pose significant challenges, ongoing technological and methodological advancements are steadily expanding the utility of EPR [69]. The integration of *in situ*/*operando* approaches, coupled with artificial intelligence-assisted data processing and multimodal characterization strategies, is expected to further enhance its role in catalysis research.

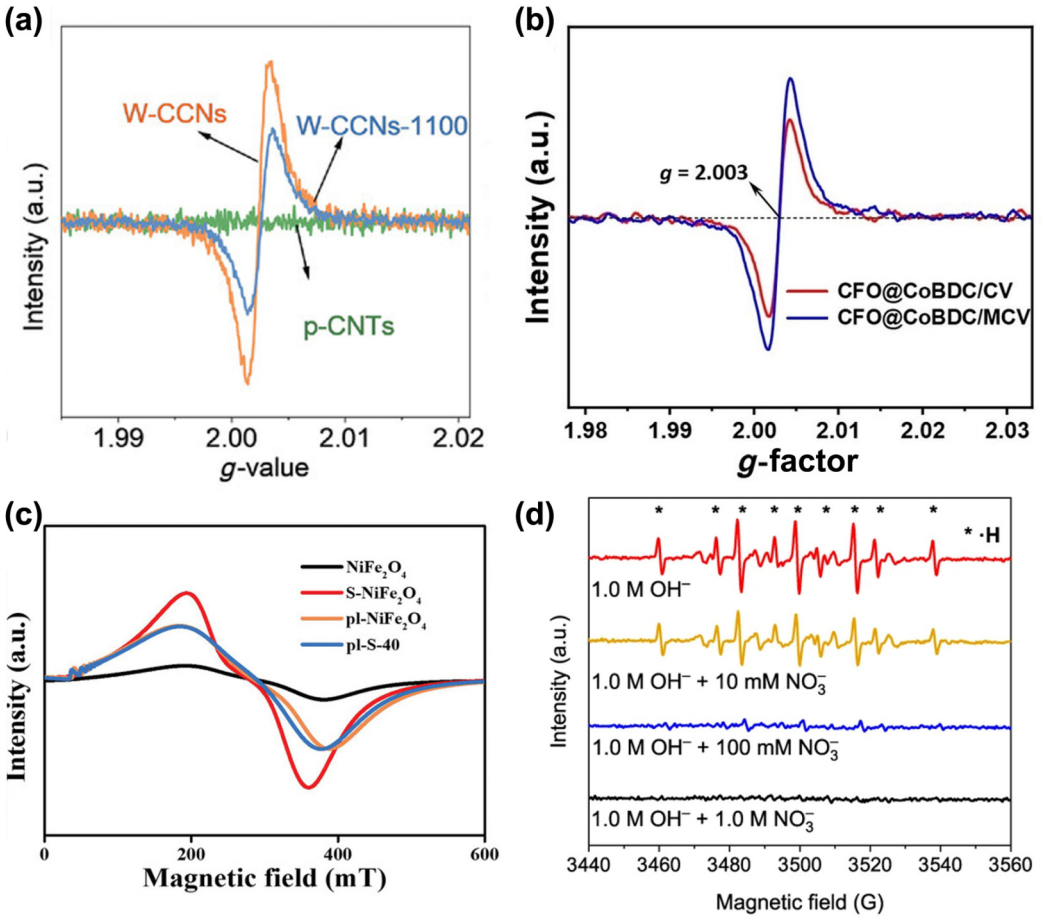

Figure 7 (a) and (b) EPR spectra of different catalysts. Reproduced with permission from (a) Ref. [64], © Wiley-VCH GmbH 2025 and (b) Ref. [65], © Wiley-VCH GmbH 2024. (c) ESR spectra of catalysts. Reproduced with permission from Ref. [66], © Wiley-VCH GmbH 2022. (d) ESR spectra at different NO_3^- concentrations. Reproduced with permission from Ref. [67], © Fan, K. et al. 2022.

3 Application of microscopic imaging techniques in catalysis

The essence of catalytic science lies in the in-depth exploration of the complex structure–activity relationship between the dynamic behavior of active sites and the underlying reaction mechanisms [70]. With the emergence of advanced fields like nanocatalysis and single-atom catalysis, traditional characterization techniques face significant challenges in terms of spatial resolution, temporal scale, and adaptability to varying working conditions. Microscopy, with its unique ability to image in real space, bridges the gap between macroscopic morphology and atomic-level structures, becoming a powerful tool for unraveling the "black box" of catalysis.

Transmission electron microscopy (TEM), especially high-resolution transmission electron microscopy (HRTEM) and scanning transmission electron microscopy (STEM), plays a pivotal role in catalytic research [71]. With sub-angstrom resolution, HRTEM provides precise insights into the crystal structure, active site distribution, and interface characteristics of catalysts, offering atomic-scale information critical for understanding catalytic processes. STEM combines the strengths of high-resolution imaging and energy spectrum analysis, enabling comprehensive examination of the catalyst's morphology, element distribution, and local structural changes, thus providing a new perspective on the atomic-level dynamics of catalysis.

Scanning electron microscopy (SEM), a classical technique, excels in revealing surface morphology and is especially valuable for large-scale observations [72]. SEM enables researchers to gather crucial data on the microstructure, particle size, distribution, and morphological evolution of catalyst surfaces, shedding light on surface dynamics during catalytic reactions.

Recent advancements in SEM have significantly broadened its applications in catalytic research. Notably, scanning electron microscopy coupled with energy-dispersive X-ray spectroscopy (SEM-EDS) enables simultaneous morphological imaging and elemental analysis, offering spatially resolved information on elemental distribution. This technique has demonstrated distinct advantages in mapping elemental dispersion, identifying active phases, and detecting micro- or nanoscale inhomogeneities or contaminants, thus becoming a critical tool for elucidating the microstructure of catalytic materials.

Furthermore, focused ion beam-scanning electron microscopy (SEM-FIB) has emerged as a powerful technique for site-specific sample preparation and three-dimensional structural analysis. By utilizing a focused ion beam for precise etching and milling, SEM-FIB enables cross-sectional imaging of catalyst layers, interfaces, and porous architectures, thereby facilitating in-depth investigation of internal material features. This technique has been widely applied in the study of catalyst degradation mechanisms, electrode–electrolyte interface characterization, and internal structural analysis of complex catalytic systems. Together, SEM-EDS and SEM-FIB offer

complementary insights at both compositional and structural levels, providing a multidimensional experimental foundation for comprehensively understanding catalyst behavior under realistic operating conditions.

Specifically, recent studies have employed SEM-EDS to track the dynamic migration pathways of active metals during catalytic processes, underscoring its pivotal role in revealing structure–activity relationships. Meanwhile, the integration of SEM-FIB into *in situ* catalysis research demonstrates its ability to reconstruct catalyst microstructures in three dimensions under reaction environments, providing direct visual evidence of deactivation mechanisms such as sintering and coking.

Atomic force microscopy (AFM) is another essential tool in catalytic research, offering atomic-scale surface detection capabilities [73]. AFM can measure fine details of catalyst surface morphology, roughness, mechanical properties, and local electronic characteristics with exceptional spatial resolution. When combined with other spectroscopic techniques, AFM provides a comprehensive view of both the physical and chemical properties of catalysts, enabling deeper insight into the microscopic mechanisms at play during catalytic reactions.

In order to systematically compare the capabilities of these microscopy techniques in catalysis, their main features are summarized in Table 3. This comparative analysis highlights how TEM, SEM, and AFM synergistically address catalytic challenges: TEM/STEM deciphers atomic-level structural motifs, SEM bridges micron-to-nanoscale morphology, and AFM quantifies nanomechanical and electronic properties [74]. Together, they enable a multiscale understanding of catalysts under realistic working conditions.

This section will explore the application of microscopy in catalytic research, highlighting its critical role in catalyst design, performance optimization, and reaction mechanism analysis.

3.1 TEM

As a core characterization technology in materials science, transmission electron microscopy has become an indispensable tool for revealing the essential properties of materials, thanks to its exceptional spatial resolution and ability to conduct in-depth microstructure analysis [75]. In the complex and demanding field of catalysis, TEM, along with its advanced derivatives HRTEM and STEM, offers unparalleled advantages. With the rapid development of cutting-edge areas like nanocatalysis and single-atom catalysis, the need for understanding the microstructure of catalysts has grown significantly. Traditional characterization methods, however, have faced limitations in spatial resolution, time scale, and adaptability to real-world working conditions, making it increasingly difficult to meet the high demands of catalytic science [76].

In this context, advanced TEM systems integrate high-resolution imaging with spectroscopic and *in-situ* capabilities, enabling comprehensive analysis of catalytic materials. This section will explore the latest advances and applications of TEM in catalysis science, with a particular focus on the HRTEM and STEM modes. We will discuss how these tools can reveal the atomic-level structure of catalysts, shed light on the dynamic behavior of active sites, and help elucidate the role of interface effects in determining catalytic efficiency. Additionally, we will highlight the potential of TEM technologies in the design and optimization of catalysts, as well as in the development of new catalytic materials, contributing to the ongoing progress and evolution of catalytic science.

Sui et al. provided a brief summary of the study of single atoms using advanced TEM. The typical configuration of a transmission electron microscope is shown in Fig. 8. It schematically illustrates an advanced TEM setup tailored for catalytic studies. The system consists of a high-energy electron beam directed through a series of condenser lenses, aberration correctors, and an objective lens to achieve atomic-resolution imaging. The sample is placed at the focal point, allowing detection through multiple modalities. High-angle annular dark-field scanning transmission electron microscopy (HAADF-STEM) is used to acquire *Z*-contrast images that reveal atomic positions with high sensitivity. Scanning transmission electron microscopy-energy dispersive X-ray spectroscopy (STEM-EDS) enables spatially resolved elemental mapping, while scanning transmission electron microscopy-electron energy loss spectroscopy (STEM-EELS) offers insights into the electronic structure and chemical bonding of elements, as demonstrated in the right-side panels. In standard TEM operation, the electron beam is adjusted to parallel light and projected directly onto the sample. In contrast, in STEM mode, the electron beam is highly focused into a tiny probe that scans and interacts with a specific area of the sample [77].

Zhao et al. proposed an innovative self-assembly method implemented on the surface of droplets to synthesize asymmetric carbon hemispheres with unique jellyfish-like morphology and radial multi-chamber mesoporous structure (Fig. 9). They cleverly used TEM characterization technology to deeply explore the potential of different amphiphilic triblock copolymers as templates in manipulating micelle structure. Through this systematic manipulation method, they successfully achieved the synthesis of a variety of novel asymmetric nanostructures, including eggshell-shaped, lotus-shaped, jellyfish-shaped, and mushroom-shaped morphologies. This research result not only highlights the unique role of TEM in revealing the powerful function of template method in nanostructure synthesis, but also opens up new horizons and

Table 3 Comparison of characteristics among TEM/STEM, SEM, and AFM, covering resolution, key functions, catalytic insights, and limitations

Feature	TEM/STEM	SEM	AFM
Resolution	0.1–0.2 nm (for atomic columns)	1–10 nm (for surface imaging)	0.01 nm (vertical resolution) 0.2 nm (lateral resolution)
Key functions	Enables crystal lattice imaging Enables EDS elemental mapping Enables electron diffraction	Facilitates large-area surface imaging Performs electron backscatter diffraction (EBSD) phase analysis	Conducts nanomechanical mapping Measures charge distribution Allows for molecular manipulation
Catalytic insights	Provides insights into active site coordination Reveals interface defects Tracks atomic scale structural evolution	Characterizes particle size/distribution Assesses surface porosity Investigates fracture mechanisms	Measures surface roughness Evaluates local stiffness variations Monitors adsorption dynamics
Limitations	Prone to beam-sensitive sample damage Involves complex sample preparation	Restricted to surface topology analysis Requires conductive coating	Slow scanning speed Suffers from thermal drift artifacts

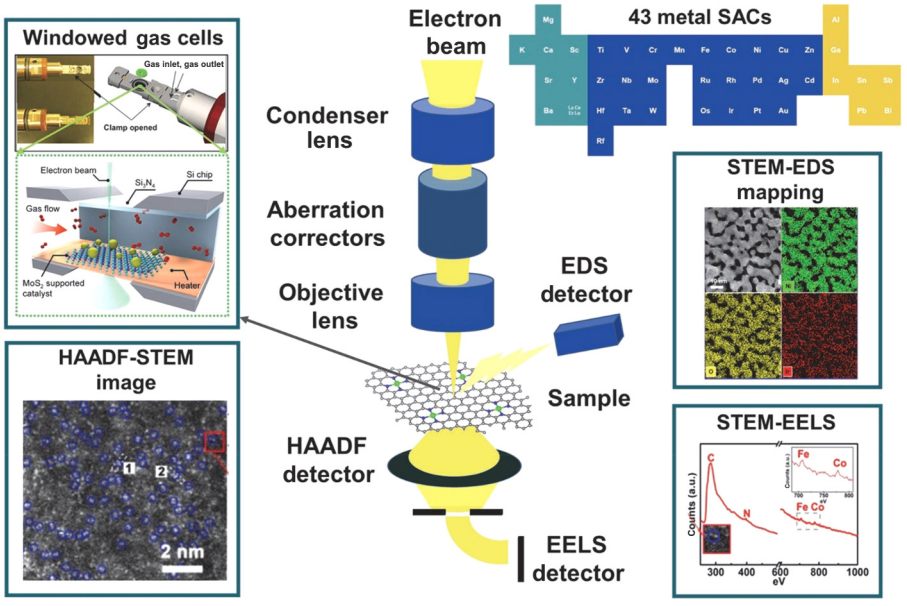

Figure 8 Typical structure of transmission electron microscope. Reproduced with permission from Ref. [77], © Jilin University, The Editorial Department of Chemical Research in Chinese Universities and Springer-Verlag GmbH 2022.

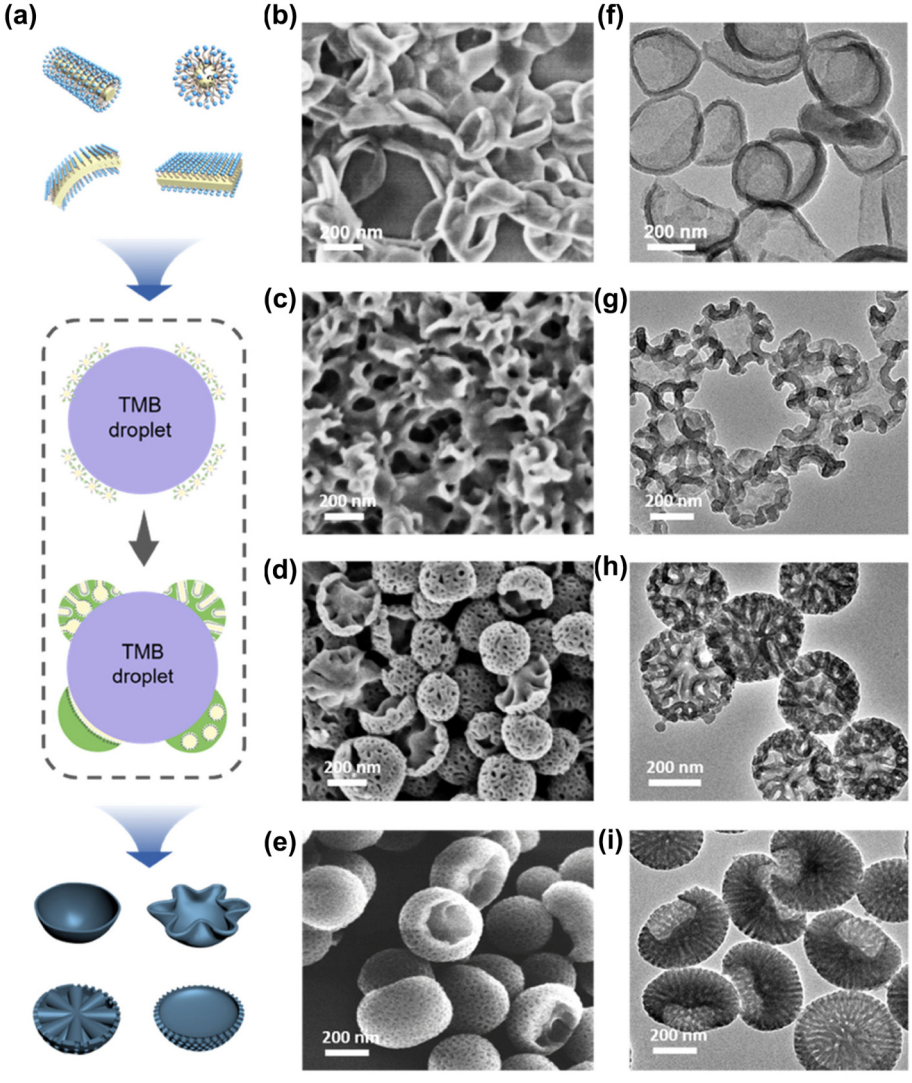

Figure 9 (a) Schematic diagram of interface self-assembly of different structures. (b)–(i) Synthesized SEM and TEM images of asymmetric mesoporous hemispheres. Reproduced with permission from Ref. [78], © American Chemical Society 2022.

paths for scientists in the field of designing and preparing nanomaterials with complex morphology and functions, highlighting the indispensability of TEM in promoting the progress of nanotechnology [78].

Hou's study employed TEM and HRTEM image analysis to reveal the phase transition mechanism of graphite under different stress conditions (Fig. 10). When *z*-axis stress dominates, graphite maintains a straight layered microstructure and directly transforms into hexagonal diamond, forming van der Waals and coherent interfaces. In contrast, when *x*-axis and *y*-axis stresses dominate, the graphite sheet compresses and deforms into a serrated microstructure, preferentially transforming into thermodynamically stable cubic diamond (Figs. 10(b)–10(e)). Due to the bending of the graphite sheet, the interface relationship becomes random, although a coherent interface can still be observed. These findings are consistent with simulation results, confirming the direct transition from graphite to both hexagonal and cubic diamond phases [79].

HRTEM generates phase contrast images through interference effects caused by the phase difference between diffracted beams and the transmitted beam [80]. For instance, Liu's research group successfully stabilized Frank's partially dislocation-strained IrNi alloy in a N-doped carbon matrix by combining dislocation formation and solid solution strengthening (Fig. 11). Using HRTEM, the researchers clearly identified two-dimensional lattice fringe features. Fast Fourier transform (FFT) of the image further revealed the dislocation defects in the IrNi alloy, showing a wide distribution of dislocations. This finding is crucial for understanding the electronic structure and chemical microenvironment of the alloy. Additionally, STEM was employed to analyze the IrNi/N-C at the atomic level. The alternating distribution of Ir and Ni atoms is clearly observed, suggesting the IrNi alloy adopts a typical face-centered cubic (fcc) crystal structure. Both HRTEM and STEM characterization provided strong experimental support for the proposed theory [81].

While conventional TEM has long served as a cornerstone for catalyst characterization by providing atomic-resolution images of crystal lattices, defect structures, and nanoparticle morphologies, its dependence on *ex-situ*, post-reaction analyses presents significant limitations [82]. The static imaging paradigm inherently overlooks transient states and dynamic processes that define catalytic functionality under operational conditions—such as metastable intermediates, including adsorbed reactants and transient surface reconstructions—while also introducing environmental artifacts, since ultrahigh vacuum environments and room-temperature measurements diverge from realistic catalytic conditions, such as high-pressure gas reactions or electrochemical interfaces. Additionally, prolonged electron exposure can induce alterations, potentially modifying catalyst structures and thereby confounding mechanistic interpretations. To overcome these constraints, researchers have pioneered *in situ* TEM methodologies that integrate real-time reaction control with atomic-scale imaging through the incorporation of miniaturized gas/liquid cells, heating stages, and electrochemical biasing systems within the TEM column, thus enabling direct visualization of catalysts during active operation [83–85].

Transmission electron microscopy has played a pivotal role in advancing catalysis science through the resolution of atomic-scale crystallographic features, defect configurations, and nanoparticle architectures [86]. However, conventional TEM analyses, typically conducted under static, *ex-situ* conditions, suffer from inherent limitations: (1) The inability to capture transient intermediates and dynamic structural evolution during catalytic reactions; (2) environmental discrepancies between observations conducted under ultrahigh vacuum and at room temperature and realistic operational settings, such as pressurized gas-phase reactions or electrochemical interfaces; and (3) potential artifacts induced by the electron beam, which may alter catalyst morphology. To address these challenges, researchers have developed *in situ* TEM platforms that integrate gas/liquid reaction cells, heating stages capable of reaching temperatures up to 1000 °C, and electrochemical biasing systems, enabling atomic-scale visualization of catalysts under *operando* conditions.

For example, Duan et al. reviewed the application of *in situ* TEM in studying strong metal–support interactions (SMSI) in

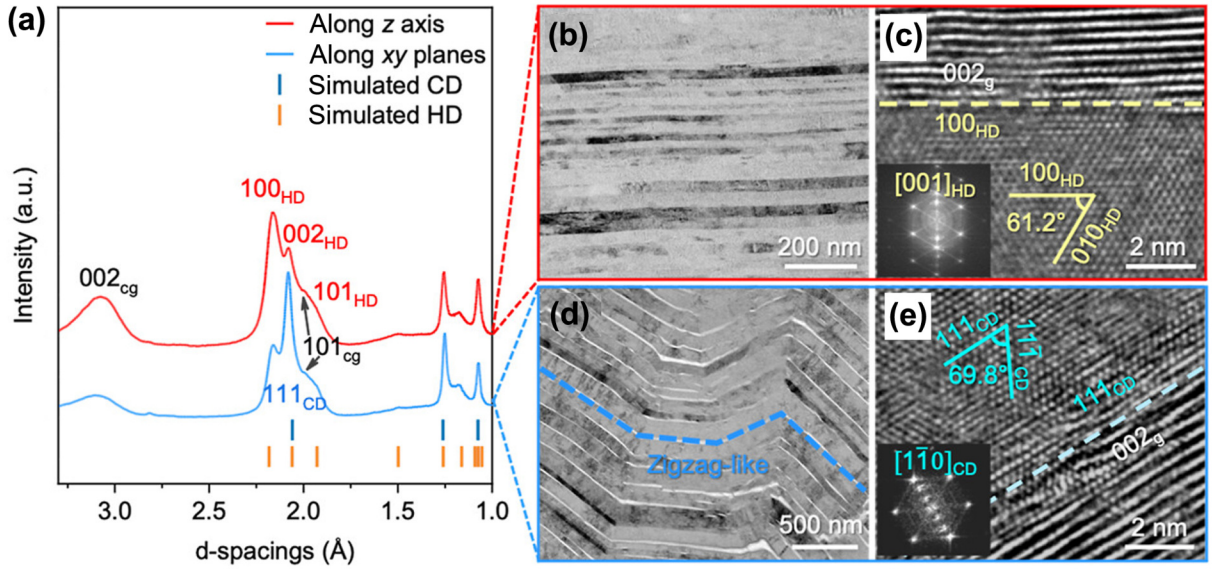

Figure 10 The transformation of graphite into hexagonal diamond and cubic diamond under hot compression. (a) XRD patterns of the samples. (b) and (c) Bright-field TEM and HRTEM images of the sample recovered from hot-compressed graphite along the *z* axis. (d) and (e) Bright-field TEM and HRTEM images of the sample recovered from hot-compressed graphite along *xy* planes. Insets in (c) and (e) are the corresponding fast Fourier transform images. Reproduced with permission from Ref. [79], © American Chemical Society 2025.

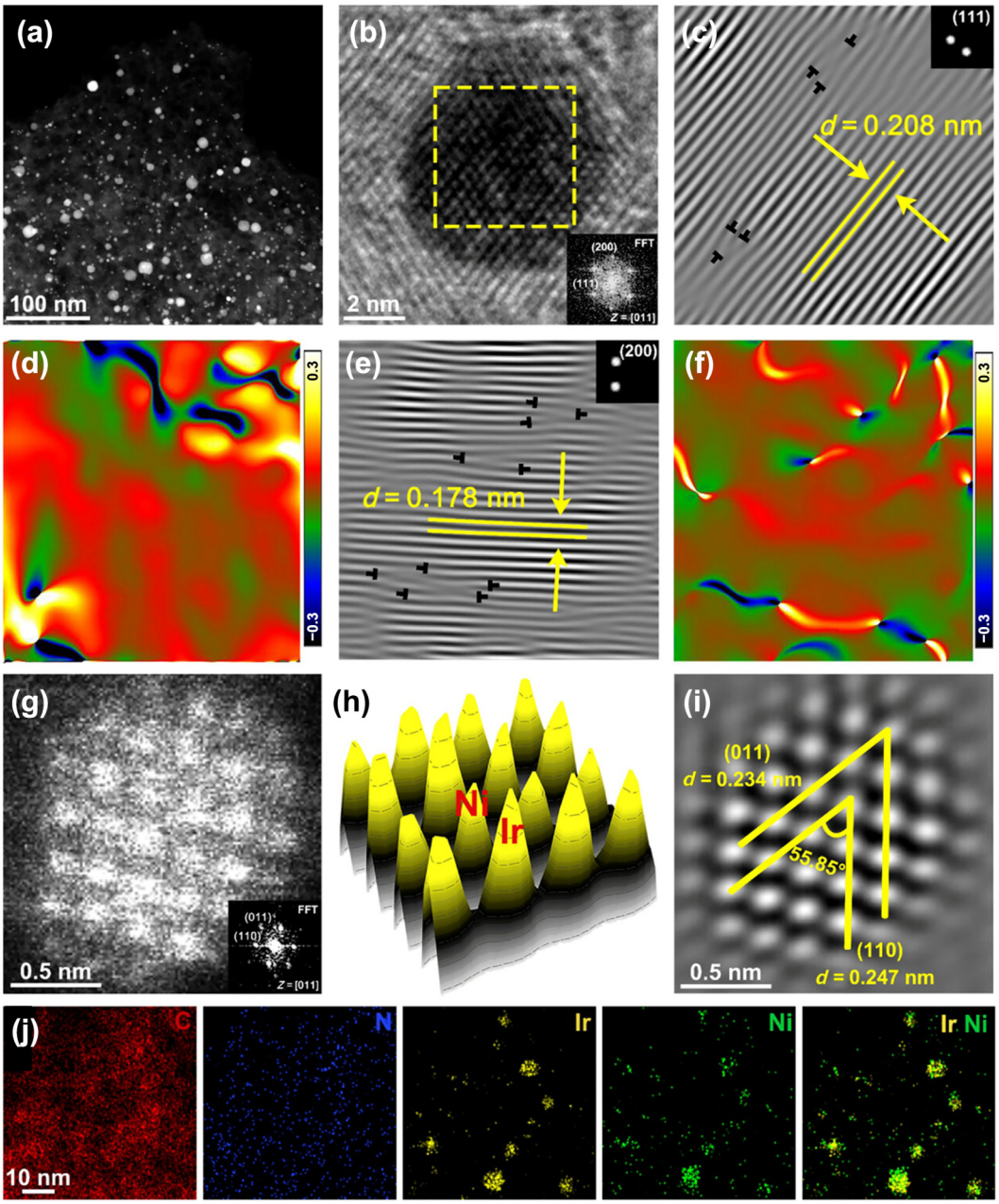

Figure 11 (a) TEM and (b) HRTEM images of IrNi/N-C composite. (c) and (e) Lattice images of the catalyst (111) and (200) planes. (d) and (f) Geometric phase analysis (GPA) of the sample on the (111) and (200) planes. (g) HAADF-STEM image of IrNi/N-C composite. (h) IrNi three-dimensional intensity distribution map. (i) High-resolution lattice image of the catalyst. (j) Sample element mapping map. Reproduced with permission from Ref. [81], © American Chemical Society 2025.

heterogeneous catalysis (Fig. 12) [87]. They systematically elucidated the latest advancements in revealing the formation dynamics of SMSI, the structural evolution during catalytic reactions, and corresponding regulation strategies, while further examining its technical merits and prospective development directions. The systematic work demonstrates that the atomic-level dynamic imaging capability of *in situ* TEM affords a unique vantage point for investigating the spatiotemporal evolution of SMSI, although its potential in complex reaction systems remains to be validated through representative catalytic cases. Based on this, Tang et al. conducted an in-depth investigation into the dynamic behavior of oscillating Pd nanocatalysts during methane oxidation, employing *in situ* environmental TEM technology, and successfully captured a direct correlation between active site reconstruction and instantaneous changes in catalytic activity under reaction conditions. Their investigation not only observed, for the first time, the periodic lattice expansion and contraction phenomenon of Pd catalysts during redox cycles but also integrated DFT calculations to elucidate the microscopic mechanism by which fluctuations in surface oxygen adsorption energy drive activity oscillations [88].

Although TEM offers the unique advantage of atomic-level resolution, it still encounters three inherent challenges in nanocatalysis research: (1) stringent ultra-thin sample preparation requirements (typically below 100 nanometers), which limit the investigation of complex catalytic systems; (2) interactions between high-energy electron beams and materials that readily induce lattice

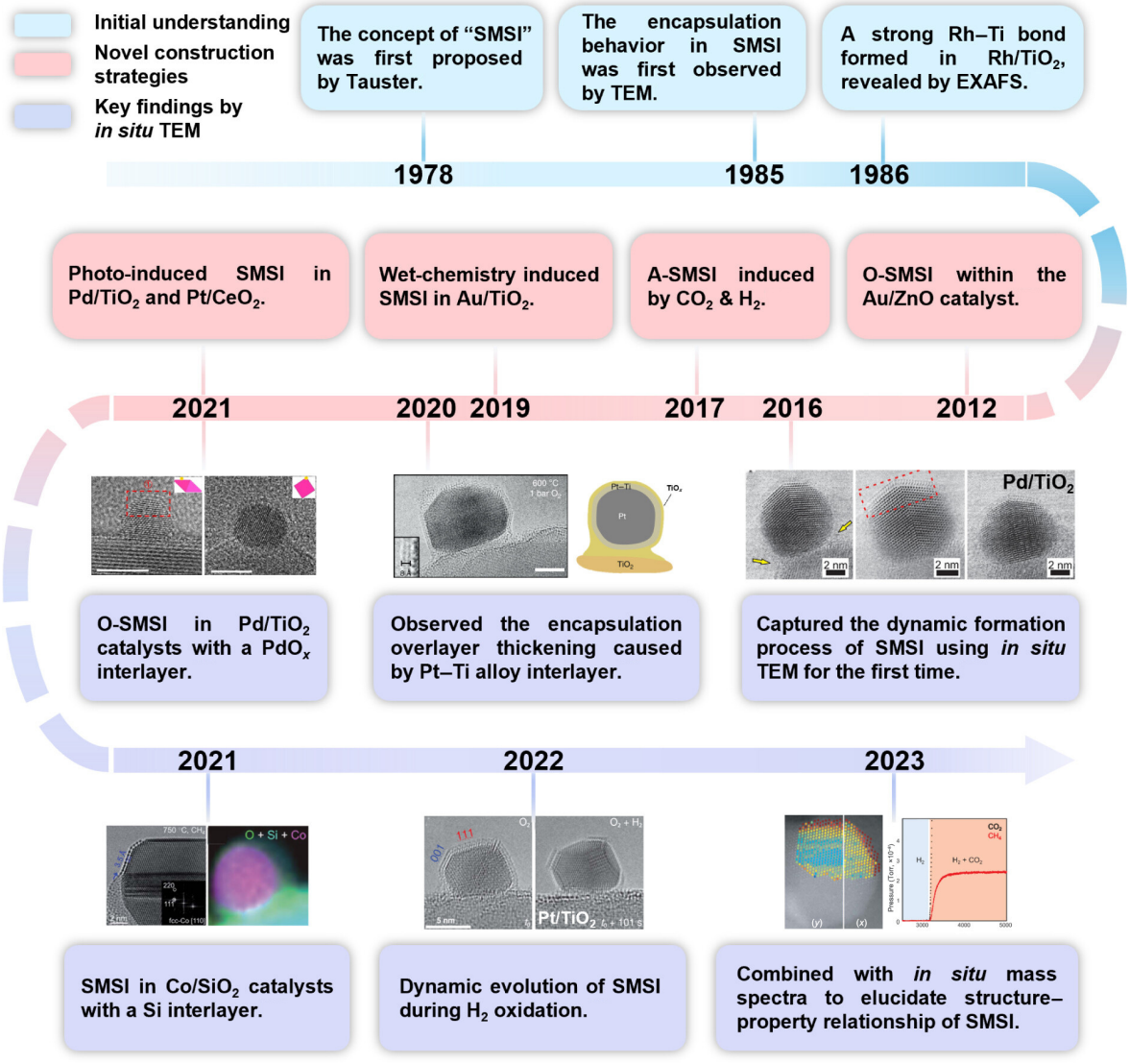

Figure 12 The history of key findings in the field of SMSI, where the representative developments of *in situ* TEM investigations are highlighted. Reproduced with permission from Ref. [87], © Wiley-VCH GmbH 2024.

damage and alter surface chemical states, thereby complicating the precise analysis of intrinsic reaction mechanisms; and (3) high-vacuum operating conditions and low-temperature sample loading constraints that hinder the capture of dynamic evolution behaviors during actual catalytic processes. To overcome these technical bottlenecks, researchers proposed integrating TEM with SEM to establish a multimodal collaborative characterization platform.

3.2 SEM

SEM is a classic and widely used characterization technique in materials science, particularly in catalysis. With its high spatial resolution, SEM provides precise observations of surface morphology and microstructure, making it an indispensable tool for studying catalysts [89]. Compared to traditional optical microscopes, SEM can achieve high magnifications and generate detailed images of sample surface characteristics by scanning the sample and detecting secondary and reflected electron signals produced by the interaction between the electron beam and the sample.

In catalytic research, SEM is extensively applied to characterize the surface morphology and structure of catalysts, especially in their synthesis, modification, and failure processes [90, 91]. By examining the surface properties of catalysts, researchers can gather vital information, such as particle size, morphology, distribution, and surface roughness. These characteristics are closely linked to the distribution of active sites and catalytic performance. As functionalized catalysts and nanocatalysts continue to advance, SEM plays a crucial role in studying the microstructure of catalysts, including the evaluation of particle agglomeration behavior and surface modifications. SEM's unique ability to visualize these features provides significant insight into catalyst design and performance optimization.

Zhao et al. pioneered a highly efficient, surfactant-free synthesis strategy to precisely control the morphology of Cu_2O nanocrystals (Fig. 13). To verify and analyze the synthesized Cu_2O nanocrystals in detail, the authors employed SEM as a key characterization tool. The SEM images provided critical insights into the morphology and structural features of the Cu_2O nanocrystals, as demonstrated in their work [92].

Although conventional SEM is widely employed for surface

morphology and compositional analysis, its requirement for high vacuum conditions and conductive sample preparation significantly limits its applicability, particularly in dynamic, real-environment studies [93]. To address these limitations and enable the real-time tracking of materials under operational conditions, *in-situ* scanning electron microscopy has been developed [94]. This technique allows observation of non-conductive samples in controllable gas or liquid environments, greatly expanding the capabilities of SEM in materials research. A comparative summary of the main features of conventional SEM and *in-situ* SEM is presented in Table 4.

With its unique advantages in visualizing dynamic processes under multifield coupling conditions, *in-situ* SEM has emerged as a powerful tool for investigating reaction mechanisms in catalysis, electrochemistry, nanomaterials, and other complex systems. For the first time, researchers at Shizuoka University in Japan employed LiPON ($Li_{3.3}PO_{3.8}N_{0.22}$) as a solid-state electrolyte and copper as the current collector to enable *in-situ* SEM observation of the electrochemical deposition and stripping behavior of metallic lithium at the Cu|LiPON interface. *In-situ* SEM dynamic imaging revealed that during lithium deposition at a current density of 50 μA·cm^{-2}, the initial nucleation sites of lithium were sparsely distributed across the LiPON|Cu interface. Subsequently, in localized regions, lithium grew through the Cu film from pre-deposited sites. Ultimately, most of the deposited lithium evolved into micron-sized needle-like structures. These results provide valuable insight into the interfacial dynamics of solid-state lithium metal batteries and highlight the utility of *in-situ* SEM in visualizing nucleation and growth behaviors at buried interfaces [95]. A representative study utilized an *in-situ* micro/nano SEM platform coupled with an electrochemical workstation to systematically investigate lithium deposition behavior on ten metal substrates in a solid-state battery with $Li_{1.5}Al_{0.5}Ge_{1.5}P_3O_{12}$ (LAGP) as the solid electrolyte [96]. The work revealed distinct out-of-plane dendritic Li growth on Cu, Ti, Ni, Bi, and Cr and in-plane particulate deposition on In, Ag, Au, Pd, and Al. The anisotropic growth rate on Cu reached 262 nm·s^{-1}, nearly 14 times higher than the isotropic growth on In. The study also visualized alloying kinetics prior to deposition, demonstrating the role of metal–Li affinity and lattice compatibility in governing Li nucleation and lateral growth. This case highlights how *in-situ* SEM can capture dynamic interfacial evolution and provide quantitative insight, offering a valuable reference for *in-situ* observation of catalytic or electrochemical processes.

In this section, we provided a comprehensive discussion on the applications and advantages of both traditional SEM and *in-situ* SEM for the microscopic observation of material interfaces. By employing *in-situ* SEM to monitor the deposition and dissolution of metallic lithium at the interface between the solid electrolyte and copper current collector, we not only elucidated the growth behavior and morphological evolution of lithium across different regions but also established a direct microstructural foundation for the design of solid-state batteries. These findings lay a robust

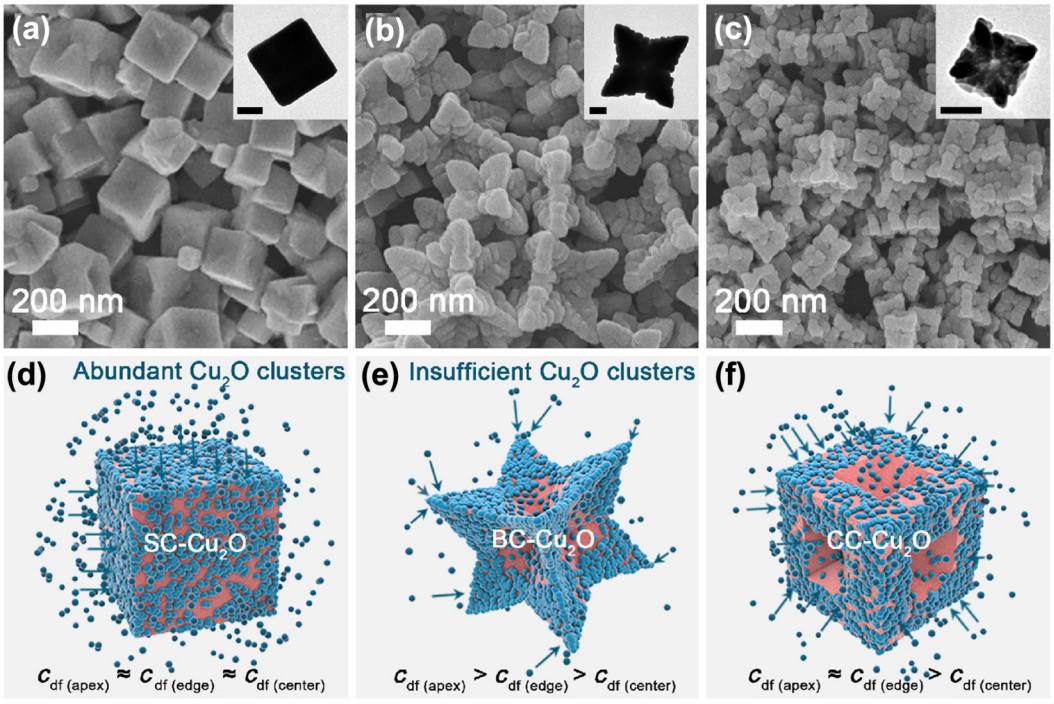

Figure 13 SEM images of Cu_2O nanocrystals growing under the following different conditions: (a) $c(Cu^{2+})$ = 625 μM, (b) $c(Cu^{2+})$ = 312.5 μM, and (c) N_2H_4 injection speed of 250 μL·min^{-1}. (d)–(f) Models corresponding to SEM images. Reproduced with permission from Ref. [92], © American Chemical Society 2022.

Table 4 A comparative table of characteristics between SEM and *in-situ* SEM

Characteristics	SEM	*In-situ* SEM
Working environment	High vacuum	Controllable gas/liquid
Sample limitations	Requires conductive treatment	Supports non-conductive samples
Dynamic observation capability	Static or extremely low-speed changes	Real-time tracking
Application scenarios	Surface morphology, composition analysis	Dynamic processes under multifield coupling

groundwork for further optimizing battery interfacial reactions and enhancing overall electrochemical performance, while demonstrating the significant potential of *in-situ* SEM in investigating complex kinetic processes [97]. Looking ahead, continual advancements in *in-situ* characterization techniques are expected to deepen our understanding of interfacial reaction mechanisms, thereby driving progressive developments in new energy materials and devices.

3.3 AFM

AFM is a high-resolution surface characterization technique that can accurately measure the morphology, mechanical properties, and local structure of catalysts at the nanoscale [98]. Compared with traditional microscopy techniques, AFM not only provides surface morphology images, but also measures the hardness, roughness, and elastic modulus of the surface, revealing the surface characteristics and structure of the catalyst. In catalytic research, AFM is widely used to observe the microstructure, surface defects, nanoparticle aggregation behavior, etc. of catalysts, especially *in situ* monitoring of surface changes during the catalytic process. Combined with other characterization techniques, AFM provides multidimensional data for the design and optimization of catalysts, helping to understand the catalytic reaction mechanism, catalyst failure, and regeneration process. Wan et al. employed *in situ* electrochemical AFM to investigate the evolution of surface morphology on Pt nanoparticle electrodes in lithium-oxygen batteries during the charge and discharge cycles (Fig. 14). They observed significant morphological changes, including an increase in the diameter of Pt nanoparticles and the formation and expansion of cracks, and established a direct correlation between these morphological transformations and the electrode's catalytic activity. Their findings provided crucial evidence and theoretical insights into the mechanism underlying the degradation of catalytic cathode performance, thereby contributing to the development of high-performance lithium-oxygen batteries [99].

The researchers utilized advanced AFM characterization technology to investigate the dynamic evolution of the interface between Mo clusters and $Ti_3C_2T_x$ carriers during the hydrogen evolution reaction (HER). In this study, nitrogen-doped molybdenum atomic clusters (Mo ACs) were supported on $Ti_3C_2T_x$ and examined as a model catalyst. By employing AFM, the researchers were able to monitor, *in situ*, the changes in surface morphology during the HER process. AFM characterization not only revealed the dynamic reorganization of Mo clusters during the catalytic reaction but also established a direct correlation between this structural evolution and HER activity. These findings highlight the potential of AFM as a powerful tool for gaining atomic-level insights into the interactions between catalysts and their supports in electrochemical reactions, particularly in elucidating the relationship between catalyst structure and performance [100].

In summary, TEM, SEM, and AFM each offer unique perspectives on catalyst morphology, surface structure, and topography. TEM provides high-resolution insights into

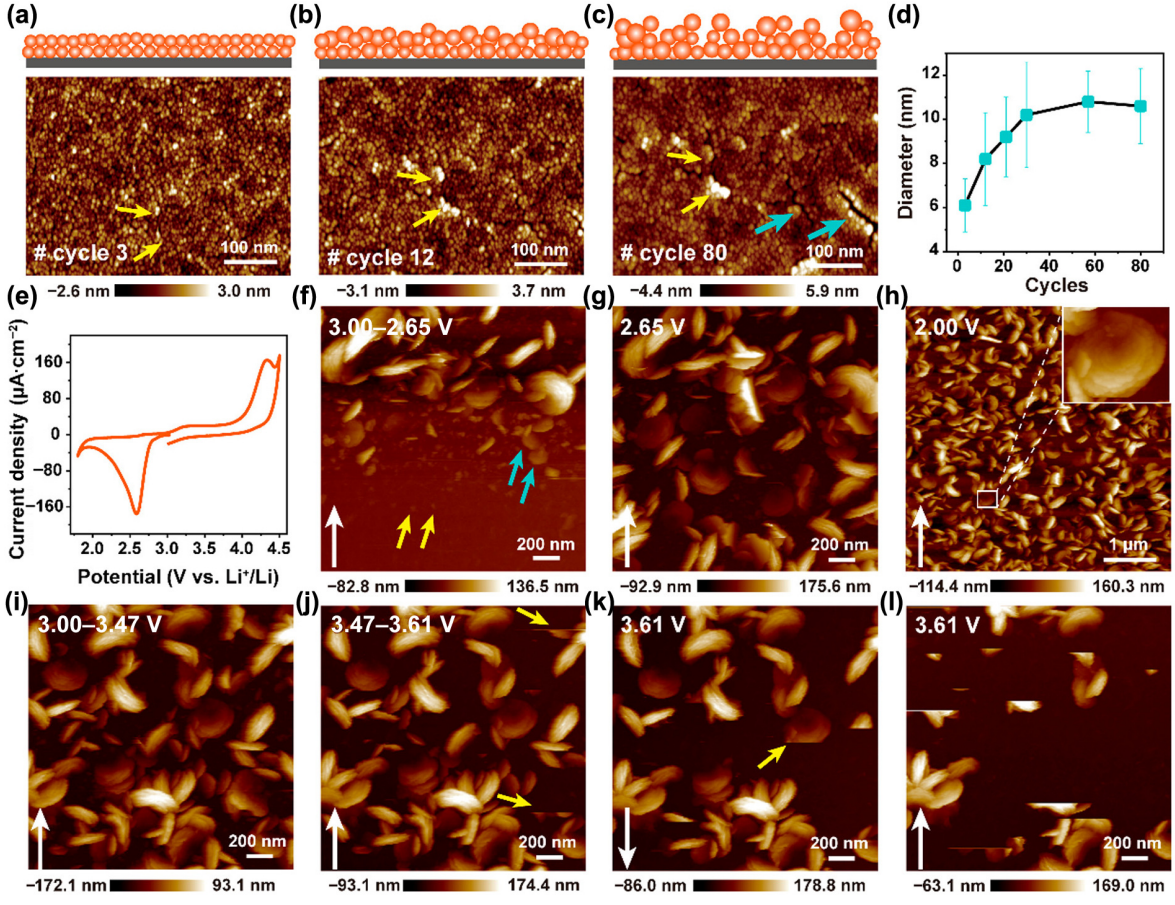

Figure 14 Schematic diagrams and AFM images of the Pt nanoparticle electrode after (a) 3, (b) 12, and (c) 80 cycles. (d) Diagram of the change in Pt particle diameter. (e) CV curve obtained on a Pt electrode. *In situ* AFM images of ((f)–(h)) discharge and ((i)–(l)) charge at different voltages (the upper left corner indicates voltage). Reproduced with permission from Ref. [99], © American Chemical Society 2021.

crystallinity and defect structures, SEM offers versatile surface imaging and elemental mapping (when coupled with EDS), while AFM enables nanoscale topographical and mechanical characterization under ambient or liquid environments. Together, these microscopic techniques form a comprehensive toolkit for visualizing structure–activity relationships in catalytic systems.

4 Application of composition analysis techniques in catalysis

In catalytic research, the composition of the catalyst and its changes during the reaction process significantly influence its catalytic performance [101, 102]. Composition analysis technologies provide essential data for uncovering the elemental composition, valence states, structural characteristics, and dynamic evolution of catalysts under reaction conditions. Widely used techniques such as X-ray photoelectron spectroscopy (XPS), inductively coupled plasma mass spectrometry (ICP-MS), and X-ray diffraction (XRD) have become indispensable tools in catalyst design and optimization. By applying these methods, researchers can comprehensively understand the elemental composition, chemical states, and crystal structure of catalysts, while also monitoring their dynamic transformations during reactions. This information is crucial for optimizing catalyst design, improving performance, and analyzing deactivation mechanisms. As analytical technologies continue to advance, composition analysis will play an increasingly pivotal role in catalysis research, driving deeper insights and innovation in the field [7, 103, 104]. To better illustrate the characteristics and applications of these common techniques, Table 5 provides a comparative summary of XPS, XRD, and ICP-MS in terms of principles, capabilities, and limitations [105].

4.1 XPS

X-ray photoelectron spectroscopy is an advanced characterization technique widely employed in surface science and catalysis research [106]. It has become a crucial tool for investigating the surface electronic structure and reaction mechanisms of catalytic materials. XPS is based on the energy analysis of photoelectrons: by irradiating the sample surface with X-rays, the inner electrons are excited, and their kinetic energy is measured, providing key insights into the elemental composition, chemical states, and surface structure of the sample [107]. Compared to other characterization techniques, XPS offers significant advantages, including high sensitivity, the ability to analyze surface properties, and chemical state analysis. These features make it particularly well-suited for studying the surface characteristics of catalysts and the surface changes that occur during reactions [108–110].

In catalysis, the surface structure, elemental distribution, and chemical state of a catalyst are critical factors influencing its activity, selectivity, and stability [111]. XPS can directly reveal the elemental composition and chemical states of each element on the catalyst surface, along with any surface species transformations that may occur during catalytic reactions. By analyzing the XPS spectrum in detail, researchers can extract valuable information regarding the distribution of active sites, redox state changes, and potential intermediates or surface reactants involved in the reaction [112]. Consequently, XPS has become an indispensable tool for elucidating the relationship between catalyst surface structure and catalytic performance.

This section will explore the unique advantages of XPS in the analysis of catalyst surface characteristics and the process of catalyst deactivation, aiming to provide an important characterization method for further understanding of catalytic reactions. Taking the Cu-Cu_2O and Ni_2P composite catalyst as an example (Figs. 15(a)–15(c)), XPS analysis clearly shows the process of electron transfer from Ni to Cu and P [113]. This finding was confirmed by the shift of specific peaks in the Cu 2p, Ni 2p, and P 2p spectra. In addition, the XPS results further confirmed the successful construction of the heterogeneous interface and pointed out that this interface structure effectively regulates the electronic structure of the catalyst, which may have a positive effect on improving the efficiency of the electrocatalytic reduction of nitrates to ammonia. Therefore, as an advanced characterization method, XPS plays an irreplaceable role in the research in the field of catalysis and provides strong support for a deep understanding of the activity, selectivity, and stability of catalysts (Figs. 15(d)–15(g)). In terms of catalyst deactivation, XPS analysis played a key role in revealing the electrocatalytic performance and catalyst deactivation mechanism of SnO/$NiCo_2O_4$/CC composite materials. By accurately identifying the changes in element valence states through XPS, researchers found that the reduction reaction of $NiCo_2O_4$ during the catalytic process protected SnO from being destroyed, significantly improving its anti-deactivation ability, providing an important theoretical basis for optimizing the structure of the composite material, improving the catalytic performance and stability, and expanding the application potential of the composite material in the field of electrocatalysis [114].

Table 5 Comparison of common characterization techniques used in catalyst composition analysis

Characterization technique	XPS	ICP-MS	XRD
Principle	The photoelectrons emitted by X-ray irradiation of the sample are used to analyze the surface elemental composition and chemical state	Ionizes the sample using plasma and detects elemental species and concentrations via mass spectrometry	Analyzes crystal structures through diffraction patterns generated by X-rays interacting with the crystal lattice
Core information	Surface elemental composition, chemical states	Elemental types and concentrations	Crystallographic structure
Detection depth	Surface-sensitive	Entire sample	Bulk-sensitive
Sample requirements	Solid samples	Liquid solutions or solid samples	Powdered or bulk solid samples
Advantages	Capable of identifying oxidation states High surface sensitivity	Extremely high sensitivity Capable of multi-element analysis	Precise crystallographic analysis Non-destructive measurement
Limitations	Only suitable for surface analysis Requires conductive or coated samples for insulating materials	Destructive testing Incapable of providing chemical state information	Cannot analyze amorphous materials Lower sensitivity to minor phases

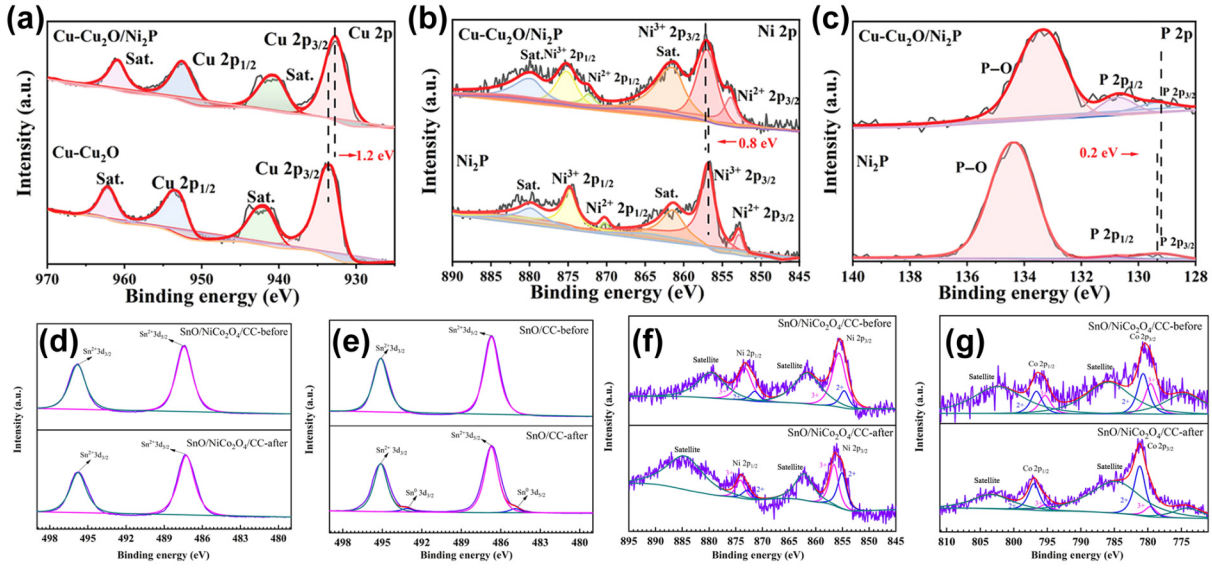

Figure 15 High-resolution XPS spectra of Cu-Cu_2O/Ni_2P, Ni_2P, and Cu-Cu_2O: (a) Cu 2p, (b) Ni 2p, and (c) P 2p. Reproduced with permission from Ref. [113], © Wiley-VCH GmbH 2025. (d)–(g) XPS spectra of the catalyst before and after reaction. Reproduced with permission from Ref. [114], © Elsevier B.V. 2023.

4.2 ICP-MS

ICP-MS is a highly sensitive elemental analysis technique extensively used in the characterization and research of catalytic materials [115]. Combining the advantages of inductively coupled plasma (ICP) and mass spectrometry (MS), ICP-MS provides both qualitative and quantitative analysis at the elemental level, making it particularly effective for detecting low-concentration elements in catalysts. This technique not only allows for precise determination of the catalyst's elemental composition but also facilitates the analysis of elemental changes during catalytic reactions and the identification of catalytic active sites.

Thomas et al. employed online ICP-MS to investigate catalyst degradation by tracking the separation or dissolution of nanoparticles into metal ions [116]. Additionally, the Marcus research team utilized ICP-MS's exceptional sensitivity, multi-element simultaneous detection capability, and rapid analysis speed to evaluate the OER activity and stability of mixed Ir-TiO_x catalysts across various compositions. By coupling ICP-MS with a scanning flow cell, researchers not only ensure accurate measurement of catalyst composition but also enable continuous flow analysis of samples. This integration plays an indispensable role in gaining deeper insights into catalyst performance, accelerating optimization screening, and assessing long-term stability [117].

4.3 XRD

XRD is a fundamental characterization technique extensively utilized in materials science, physical chemistry, and catalysis research [118–120]. By analyzing the diffraction pattern generated when a sample is irradiated with X-rays, XRD provides valuable information about the crystal structure, phase composition, grain size, and crystal defects of the material. It is an essential tool in the research and development of catalysts. In catalysis, XRD is particularly effective for studying the crystal structure, phase transition behavior, and dynamic changes in catalytic materials during reactions. This capability enables a deeper understanding of the relationship between the catalyst's structural properties and its catalytic performance.

XRD is a crucial technique for characterizing catalysts, providing detailed information on crystal structure, phase composition, particle size, structural modifications, and defects. One of its key applications is the analysis of the crystal structure of catalysts. For instance, in the study of Ir-Co_3O_4 electrocatalysts, XRD analysis revealed that the introduction of Ir did not significantly alter the lattice structure of Co_3O_4, suggesting that Ir predominantly exists in an atomically dispersed form (Fig. 16(a)) [121]. Secondly, XRD can reveal the composition and particle size information of different phases in the catalyst. No obvious Ni crystal peak was observed in the Ni catalyst, indicating that Ni exists in the form of single atoms or small nanoparticles, which helps to understand the dispersion state of metals in the catalyst (Fig. 16(b)) [122]. XRD is also highly effective in analyzing structural changes and the effects of doping in materials. For example, the XRD spectrum of a porous carbon catalyst doped with boron (B) exhibits noticeable peak-to-valley shifts, indicating that boron doping induces structural modifications and increases disorder within the material (Fig. 16(c)) [123]. Through XRD, researchers can also observe the phase changes of the catalyst. For example, the increase of FeCoNi content causes the catalyst to transform from perovskite phase to perovskite–rock salt mixed phase, reflecting the interaction and structural changes between metal elements [124] (Fig. 16(d)). Finally, XRD can detect defects and lattice strain in the catalyst. For example, in the XRD pattern of the ZIS-*x* catalyst, the downward shift of the (006) peak indicates that the defects cause the lattice to stretch, thus affecting the structure of the catalyst (Fig. 16(e)) [125]. These XRD analyses help researchers gain a deeper understanding of the relationship between catalyst structure and performance, and provide a scientific basis for catalyst design and optimization. Building upon conventional structural characterization under static conditions, *in situ* XRD has emerged as a powerful extension, enabling real-time monitoring of transient phase transformations and lattice dynamics under *operando* environments. This technique is exemplified by its ability to track the structural evolution of materials such as LMO and Hf-LMO during initial charge-discharge processes, providing critical insights into their dynamic behavior and stability (Fig. 16(f)) [126].

In summary, XRD serves as a versatile and indispensable

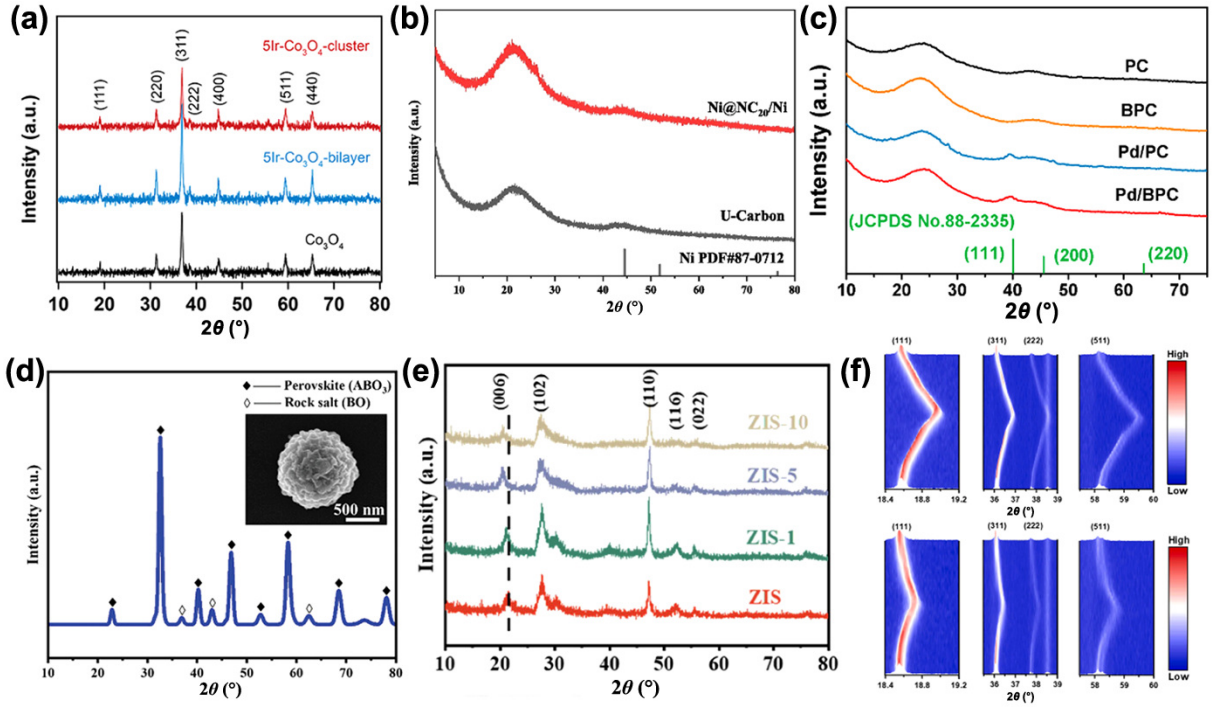

Figure 16 (a) XRD patterns of pristine Co_3O_4, 5Ir-Co_3O_4 bilayer, and 5Ir-Co_3O_4 cluster. Reproduced with permission from Ref. [121], © American Chemical Society 2025. (b) XRD patterns of Ni@NC_{20}/Ni and U-carbon, with the standard diffraction peaks of metallic Ni (PDF#87-0712) shown for reference. Reproduced with permission from Ref. [122], © Elsevier B.V. 2025. (c) XRD patterns of PC, BPC, Pd/PC, and Pd/BPC. The reference peaks of metallic Pd (JCPDS No. 88-2335) are indicated. Reproduced with permission from Ref. [123], © Liu, H. et al. 2024. (d) XRD pattern of the perovskite–rock salt composite, where the diffraction peaks indexed to the perovskite (ABO_3) and rock salt (BO) phases are marked. The inset shows a representative SEM image of a single particle. Reproduced with permission from Ref. [124], © Wiley-VCH GmbH 2025. (e) XRD patterns of ZIS, ZIS-1, ZIS-5, and ZIS-10, illustrating the phase evolution with increasing treatment level. The main diffraction peaks are indexed. Reproduced with permission from Ref. [125], © American Chemical Society 2025. (f) *In situ* XRD contour plots showing the evolution of characteristic diffraction peaks during the reaction, where the color scales represent the diffraction intensity. Reproduced with permission from Ref. [126], © Elsevier Ltd. 2024.

technique in catalytic research, offering both static and dynamic insights into the crystal structure, phase behavior, and defect states of catalyst [127]. By combining *ex situ* and *in situ* XRD analyses, researchers can not only decode the structural basis of catalytic performance but also elucidate the evolution of active phases under reaction conditions. This structural information lays a critical foundation for the rational design, precise modulation, and performance enhancement of advanced catalytic materials, thereby propelling innovation in catalyst development and application [128].

5 Conclusions and perspectives

In the field of catalysis, advanced characterization techniques—such as spectroscopy, microscopy, compositional analysis, and dynamic characterization are essential for catalyst design, performance enhancement, and the elucidation of reaction mechanism [129]. Despite their great potential in scientific research, these techniques face significant challenges and limitations in practical applications, necessitating further development and refinement. One of the major bottlenecks is the limitation in spatial resolution. Although techniques like XAS and TEM provide detailed insights into the local structure of catalysts, their resolution remains inadequate for the precise investigation of single-atom or nanoscale catalysts. This shortfall hinders the accurate observation of subtle structural changes at the atomic level. Furthermore, Raman and infrared spectroscopy often suffer from overlapping signals in complex, high-density catalytic systems, complicating the accurate identification of surface reactions. Another challenge lies in the need to operate many advanced characterization techniques under extreme conditions, such as high temperature, high pressure, or high vacuum which imposes stringent demands on equipment stability and experimental precision [130–132]. *In situ* characterization techniques, in particular, require real-time monitoring of catalysts under realistic reaction conditions, necessitating instruments with high-precision control systems and advanced data acquisition capabilities. The high cost of instrumentation and the complexity of experimental setups—especially when multiple techniques are integrated—further elevate research costs. Additionally, the growing volume of experimental data presents a pressing challenge: how to efficiently process and interpret complex datasets to extract meaningful physical and chemical insights [133].

To overcome current limitations in catalyst characterization, future research should pursue several strategic directions. In the realm of spectroscopic techniques, enhancing spatial resolution remains a primary objective. This requires the development of next-generation tools such as synchrotron-based stacked scanning imaging and single-atom X-ray imaging, which enable atomic-scale insights and multidimensional characterization of catalyst structures [134]. In parallel, integrating advanced computational approaches—such as spectral deconvolution, chemometric analysis, and surface-enhanced Raman spectroscopy—is strongly encouraged. These methods can significantly improve the identification of surface intermediates and reaction pathways,

particularly addressing spectral overlap issues commonly encountered in Raman and infrared spectroscopy. In the domain of microscopic imaging, future developments should focus on advancing aberration-corrected and cryogenic microscopy techniques capable of achieving atomic resolution while minimizing beam-induced damage. Moreover, the integration of *in situ* environmental transmission electron microscopy (ETEM) and liquid cell TEM offers valuable opportunities to observe morphological evolution and particle migration under near-*operando* catalytic conditions. Concurrently, deep learning (DL)-assisted denoising and tomographic reconstruction are expected to substantially enhance the interpretability and accuracy of microscopy data in complex catalytic environments.

Compositional analysis techniques remain fundamental for probing the elemental composition and chemical states of catalysts. However, challenges such as surface sensitivity, sample charging, matrix effects, and difficulty in quantifying trace elements still hinder their broad application in heterogeneous catalytic systems. To address these issues, the development of depth-resolved and time-resolved analysis methods is essential. Techniques such as angle-resolved X-ray photoelectron spectroscopy (ARXPS) and time-of-flight secondary ion mass spectrometry (ToF-SIMS) enable depth profiling and real-time tracking of surface species during reactions [135–137]. Enhancing quantitative reliability through standardized protocols and reference-based calibration is also crucial for improving data accuracy and reproducibility.

In situ characterization represents another vital frontier. Future work should prioritize the design of robust, multifunctional reaction cells capable of withstanding high-temperature, high-pressure, and corrosive environments, while remaining compatible with a wide range of characterization techniques. To reduce experimental complexity and cost, the development of miniaturized and modular platforms will also be essential, improving adaptability and portability across diverse catalytic systems.

The exponential growth of experimental data highlights the urgent need for AI and machine learning (ML) techniques in data processing and interpretation [138]. AI/ML models tailored to catalytic systems facilitate the extraction of structural and mechanistic insights from complex datasets, thereby accelerating catalyst discovery and performance optimization. The establishment of open-access databases and standardized data acquisition protocols will further enable intelligent characterization platforms and foster interdisciplinary collaboration.

For example, the introduction of AI offers a powerful new paradigm for processing and analyzing XAS data [139]. By constructing automated preprocessing pipelines—including principal component analysis (PCA), *z*-score normalization, outlier detection, and cluster analysis—researchers can systematically clean and standardize raw XAS datasets, laying a robust foundation for subsequent machine learning modeling. This not only enhances the accuracy and generalizability of predictive models but also accelerates the extraction of hidden relationships from experimental data, thereby addressing key challenges in structural analysis, phase identification, and performance prediction. With the rapid development of high-resolution imaging technologies, liquid-phase transmission electron microscopy (liquid-phase TEM) and SEM have become indispensable tools for visualizing material structures and dynamic transformations [140, 141]. However, such image datasets often suffer from high noise levels, strong background fluctuations, and poorly defined feature boundaries, posing major obstacles to the accurate extraction of physical and chemical parameters. The integration of AI, particularly DL methods, provides a transformative approach to high-throughput and quantitative image analysis. In the case of liquid-phase TEM, researchers have developed analysis frameworks based on U-Net convolutional neural networks, using simulated, ground-truth-labeled images for training. This strategy has dramatically improved the recognition accuracy of nanoparticle positions, morphologies, and dynamic behaviors in noisy, complex environments. Such methods have been successfully applied to elucidate the diffusion, reaction kinetics, and assembly processes of colloidal nanoparticles with diverse shapes, revealing key structural evolution features such as anisotropic interactions of nanoprisms, curvature-dependent etching of nanorods, and first-order chaining kinetics of concave cubic particles. Similarly, in SEM image analysis, deep learning models—such as convolutional neural networks (CNNs)—have demonstrated strong capabilities in automatic segmentation, pore size measurement, and network connectivity analysis in porous materials. These AI-driven methods are especially effective for analyzing materials with high structural heterogeneity and complexity, such as metal–organic frameworks (MOFs), porous carbons, and aerogels, offering repeatable, standardized, and scalable approaches for pore network quantification. The widespread adoption of AI, particularly deep learning, in the analysis of XAS, TEM, and SEM data is catalyzing a paradigm shift in materials characterization—from traditional empiricism toward high-throughput, automation, and intelligence-driven workflows. These innovations provide powerful tools for decoding complex material structures and enabling more accurate performance predictions.

In summary, catalytic reactions are central to addressing global challenges in energy conversion, green chemistry, and sustainable chemical manufacturing. The ongoing advancement of spectroscopic, microscopic, and dynamic characterization technologies offers unprecedented capabilities for catalyst design, mechanistic understanding, and performance evaluation. Although these technologies have already transformed catalysis research, practical limitations remain. Future efforts must focus on overcoming these constraints by developing more precise, efficient, and accessible characterization methods. Coupled with artificial intelligence and standardized protocols, these innovations will play a pivotal role in advancing the sustainable development of catalysis and materials science.

Data availability

Not applicable.

Acknowledgements

We gratefully acknowledge financial support by "Grassland Talents" of Inner Mongolia Autonomous Region, Young Talents of Science and Technology in Universities of Inner Mongolia Autonomous Region (No. NJYT23030), Technology Breakthrough Engineering Hydrogen Energy Field "Unveiling and Leading" Project (No. 2024KJTW0018), "Steed Plan High Level Talents" of Inner Mongolia University, Carbon Neutralization Research Project (No. STZX202218), the National Natural Science Foundation of China (No. U22A20107), Inner Mongolia Autonomous Region Natural Science Foundation (No. 2023MS02002), Guangdong Provincial Key Laboratory of Materials and Technologies for Energy

Conversion (No. MATEC2024KF011), the National Key R&D Program of China (No. 2022YFA1205201), and Inner Mongolia Autonomous Region Graduate Research Innovation Project (No. KC2024020B).

Declaration of competing interest

All the contributing authors report no conflict of interests in this work.

Author contribution statement

R. R.: Investigation and writing – original draft. K. G.: Supervision and writing – review & editing. Y. L. G.: Validation and writing – original draft. G. F. L.: Resources. L. R. Z.: Methodology and resources. Y. F. W.: Data curation and investigation. Q. N. Z.: Methodology and resources. Q. W.: Investigation and supervision. J. W. Z.: Funding acquisition, supervision, and writing – review & editing. All the authors have approved the final manuscript.

Use of AI statement

None.

References

[1] Das, S.; Pérez-Ramírez, J.; Gong, J. L.; Dewangan, N.; Hidajat, K.; Gates, B. C.; Kawi, S. Core–shell structured catalysts for thermocatalytic, photocatalytic, and electrocatalytic conversion of CO_2. *Chem. Soc. Rev.* **2020**, *49*, 2937–3004.

[2] Sharma, R.; Sharda, H.; Dutta, A.; Dahiya, A.; Chaudhary, R.; Singh, A.; Rathi, K.; Kumar, S.; Sharma, A.; Maken, S. et al. Optimizing green hydrogen production: Leveraging load profile simulation and renewable energy integration. *Int. J. Hydrogen Energy* **2023**, *48*, 38015–38026.

[3] Takagi, R.; Yamasaki, Y.; Yokouchi, T.; Ukleev, V.; Yokoyama, Y.; Nakao, H.; Arima, T.; Tokura, Y.; Seki, S. Particle-size dependent structural transformation of skyrmion lattice. *Nat. Commun.* **2020**, *11*, 5685.

[4] He, C. H.; Xia, C. F.; Li, F. M.; Zhang, J.; Guo, W.; Xia, B. Y. Rational design of oxygen species adsorption on nonnoble metal catalysts for two-electron oxygen reduction. *Adv. Energy Mater.* **2024**, *14*, 2303233.

[5] Du, C. Y.; Sheng, J. P.; Zhong, F. Y.; He, Y.; Guro, V. P.; Sun, Y. J.; Dong, F. Rational design and mechanistic insights of advanced photocatalysts for CO_2-to-C_{2+} production: Status and challenges. *Chin. J. Catal.* **2024**, *60*, 25–41.

[6] Ou, Y.; Zhang, Y. F.; Luo, W.; Wu, Y.; Wang, Y. Rational design of covalent organic frameworks for photocatalytic hydrogen peroxide production. *Macromol. Rapid Commun.* **2025**, *46*, 2401149.

[7] Anekwe, I. M. S.; Akpasi, S. O.; Enemuo, E. M.; Ashiegbu, D.; Mustapha, S. I.; Isa, Y. M. Innovations in catalytic understanding: A journey through advanced characterization. *Mater. Today Catal.* **2024**, *7*, 100061.

[8] Hu, C. J.; Hu, Y. F.; Zhang, B. W.; Zhang, H. W.; Bao, X. J.; Zhang, J. J.; Yuan, P. Advanced catalyst design strategies and *in-situ* characterization techniques for enhancing electrocatalytic activity and stability of oxygen evolution reaction. *Electrochem. Energy Rev.* **2024**, *7*, 19.

[9] Zhao, Y. G.; Adiyeri Saseendran, D. P.; Huang, C.; Triana, C. A.; Marks, W. R.; Chen, H.; Zhao, H.; Patzke, G. R. Oxygen evolution/reduction reaction catalysts: From *in situ* monitoring and reaction mechanisms to rational design. *Chem. Rev.* **2023**, *123*, 6257–6358.

[10] Faghmous, J. H.; Kumar, V. Spatio-temporal data mining for climate data: Advances, challenges, and opportunities. In *International Journal of Information Management*. Chu, W. W., Ed.; Springer: Berlin, Heidelberg, **2014**; pp 83–116.

[11] Xiao, J.; Aggarwal, A. K.; Duc, N. H.; Arya, A.; Rage, U. K.; Avtar, R. A review of remote sensing image spatiotemporal fusion: Challenges, applications and recent trends. *Remote Sens. Appl.: Soc. Environ.* **2023**, *32*, 101005.

[12] Backes, C.; Englert, J. M.; Bernhard, N.; Hauke, F.; Hirsch, A. Optical visualization of carbon nanotubes—a unifying linkage between microscopic and spectroscopic characterization techniques. *Small* **2010**, *6*, 1968–1973.

[13] Deng, J. J.; Zhang, Q. Z.; Lv, X. X.; Zhang, D.; Xu, H.; Ma, D. L.; Zhong, J. Understanding photoelectrochemical water oxidation with X-ray absorption spectroscopy. *ACS Energy Lett.* **2020**, *5*, 975–993.

[14] Wan, G.; Zhang, G. H.; Chen, J. Z.; Toney, M. F.; Miller, J. T.; Tassone, C. J. Reaction-mediated transformation of working catalysts. *ACS Catal.* **2022**, *12*, 8007–8018.

[15] Timoshenko, J.; Roldan Cuenya, B. *In situ*/*operando* electrocatalyst characterization by X-ray absorption spectroscopy. *Chem. Rev.* **2021**, *121*, 882–961.

[16] Feijóo, J.; Yang, Y.; Fonseca Guzman, M. V.; Vargas, A.; Chen, C. B.; Pollock, C. J.; Yang, P. D. *Operando* high-energy-resolution X-ray spectroscopy of evolving Cu nanoparticle electrocatalysts for CO_2 reduction. *J. Am. Chem. Soc.* **2023**, *145*, 20208–20213.

[17] Kerr, B. V.; King, H. J.; Garibello, C. F.; Dissanayake, P. R.; Simonov, A. N.; Johannessen, B.; Eldridge, D. S.; Hocking, R. K. Characterization of energy materials with X-ray absorption spectroscopy—advantages, challenges, and opportunities. *Energy Fuels* **2022**, *36*, 2369–2389.

[18] Ren, R.; Li, S. T.; Gu, Y. L.; Li, G. F.; Xue, D. D.; Liu, N.; Zhang, Y. L.; An, L.; Zhang, J. W. Methodological characterization of X-ray absorption spectroscopy in small molecule conversion processes utilizing energy catalytic nanomaterials. *Next Mater.* **2025**, *7*, 100343.

[19] Timoshenko, J.; Haase, F. T.; Saddeler, S.; Rüscher, M.; Jeon, H. S.; Herzog, A.; Hejral, U.; Bergmann, A.; Schulz, S.; Roldan Cuenya, B. Deciphering the structural and chemical transformations of oxide catalysts during oxygen evolution reaction using quick X-ray absorption spectroscopy and machine learning. *J. Am. Chem. Soc.* **2023**, *145*, 4065–4080.

[20] Yang, S.; Wei, Y.; Li, X. W.; Mao, J. N.; Mei, B. B.; Xu, Q.; Li, X. P.; Jiang, Z. Construction of high-density binuclear site catalysts from double framework interfaces at the cooling stage. *Angew. Chem.* **2023**, *135*, e202313029.

[21] Zhang, T. Y.; Jiang, J. J.; Sun, W. M.; Gong, S. Y.; Liu, X. W.; Tian, Y.; Wang, D. S. Spatial configuration of Fe–Co dual-sites boosting catalytic intermediates coupling toward oxygen evolution reaction. *Proc. Natl. Acad. Sci. USA* **2024**, *121*, e2317247121.

[22] Hui, L.; Yan, D. X.; Zhang, X. T.; Wu, H.; Li, J. Z.; Li, Y. L. Halogen tailoring of platinum electrocatalyst with high CO tolerance for methanol oxidation reaction. *Angew. Chem.* **2024**, *136*, e202410413.

[23] Chen, Y. Q.; Dong, Z.; Lai, S.; Li, Y. B.; Lv, W.; He, Y. B.; Kang, F. Y.; Liu, M. Review for advanced NMR characterization of carbon-based and metal anodes in sodium batteries. *Adv. Funct. Mater.* **2024**, *34*, 2408657.

[24] Qi, G. D.; Wang, Q.; Xu, J.; Deng, F. Solid-state NMR studies of internuclear correlations for characterizing catalytic materials. *Chem. Soc. Rev.* **2021**, *50*, 8382–8399.

[25] Lehr, M.; Paschelke, T.; Trumpf, E.; Vogt, A. M.; Näther, C.; Sönnichsen, F. D.; McConnell, A. J. A paramagnetic NMR spectroscopy toolbox for the characterisation of paramagnetic/spin-crossover coordination complexes and metal–organic cages. *Angew.*

Chem. Int. Ed. **2020**, *59*, 19344–19351.

[26] Liu, X. S.; Liang, Z. T.; Xiang, Y. X.; Lin, M.; Li, Q.; Liu, Z. G.; Zhong, G. M.; Fu, R. Q.; Yang, Y. Solid-state NMR and MRI spectroscopy for Li/Na batteries: Materials, interface, and *in situ* characterization. *Adv. Mater.* **2021**, *33*, 2005878.

[27] Khalil, I.; Rigamonti, M. G.; Janssens, K.; Bugaev, A.; Esteban, D. A.; Robijns, S.; Donckels, T.; Beydokhti, M. T.; Bals, S.; de Vos, D. et al. Atomically dispersed ruthenium hydride on beta zeolite as catalysts for the isomerization of muconates. *Nat. Catal.* **2024**, *7*, 921–933.

[28] Qu, Z. Q.; He, G. Y.; Zhang, T. J.; Fan, Y. Q.; Guo, Y. X.; Hu, M.; Xu, J.; Ma, Y. H.; Zhang, J. C.; Fan, W. B. et al. Tricoordinated single-atom cobalt in zeolite boosting propane dehydrogenation. *J. Am. Chem. Soc.* **2024**, *146*, 8939–8948.

[29] Wang, W. Y.; Xu, J.; Deng, F. Recent advances in solid-state NMR of zeolite catalysts. *Natl. Sci. Rev.* **2022**, *9*, nwac155.

[30] Ahlawat, S.; Mote, K. R.; Lakomek, N. A.; Agarwal, V. Solid-state NMR: Methods for biological solids. *Chem. Rev.* **2022**, *122*, 9643–9737.

[31] Asakura, T.; Naito, A. Structure of spider silk studied with solid-state NMR. *Adv. Funct. Mater.* **2025**, *35*, 2407544.

[32] Copéret, C.; Liao, W. C.; Gordon, C. P.; Ong, T. C. Active sites in supported single-site catalysts: An NMR perspective. *J. Am. Chem. Soc.* **2017**, *139*, 10588–10596.

[33] Arakawa, H.; Aresta, M.; Armor, J. N.; Barteau, M. A.; Beckman, E. J.; Bell, A. T.; Bercaw, J. E.; Creutz, C.; Dinjus, E.; Dixon, D. A. et al. Catalysis research of relevance to carbon management: Progress, challenges, and opportunities. *Chem. Rev.* **2001**, *101*, 953–996.

[34] Chen, L. F.; Ding, X. Z.; Wang, Z. R.; Xu, S. T.; Jiang, Q. K.; Dun, C. C.; Urban, J. J. Advances in *in situ*/*operando* techniques for catalysis research: Enhancing insights and discoveries. *Surf. Sci. Technol.* **2024**, *2*, 9.

[35] Loy, A. C. M.; Ng, W. L.; Bhattacharya, S. Advanced characterization techniques for the development of subatomic scale catalysts: One step closer to industrial scale fabrication. *Mater. Today Catal.* **2024**, *4*, 100033.

[36] Demco, D. E.; Oros-Peusquens, A. M.; Shah, N. J. Nonlinear effects in magnetic resonance localized spectroscopy and images. *Prog. Nucl. Magn. Reson. Spectrosc.* **2025**, *146–147*, 101557.

[37] De Biasi, F.; Hope, M. A.; Avalos, C. E.; Karthikeyan, G.; Casano, G.; Mishra, A.; Badoni, S.; Stevanato, G.; Kubicki, D. J.; Milani, J. et al. Optically enhanced solid-state ^{1}H NMR spectroscopy. *J. Am. Chem. Soc.* **2023**, *145*, 14874–14883.

[38] Chen, S. Z.; Zhang, L.; Li, S.; Yuan, Y. P.; Jiang, B.; Jiang, Z. X.; Zhang, X.; Zhou, X.; Liu, M. L. Detecting biomarkers by dynamic nuclear polarization enhanced magnetic resonance. *Natl. Sci. Rev.* **2024**, *11*, nwae228.

[39] Elipe, M. V. S. Advantages and disadvantages of nuclear magnetic resonance spectroscopy as a hyphenated technique. *Anal. Chim. Acta* **2003**, *497*, 1–25.

[40] Simmler, C.; Napolitano, J. G.; McAlpine, J. B.; Chen, S. N.; Pauli, G. F. Universal quantitative NMR analysis of complex natural samples. *Curr. Opin. Biotechnol.* **2014**, *25*, 51–59.

[41] Murugaperumal, P.; Rajendran, P.; Nallathambi, S.; Ayyanar, S.; Perdih, F.; Chellappan, S. Oxalohydrazide-based chemosensor for detection of Cu^{2+}/Fe^{3+} ions and its application in live cell imaging. *ChemistrySelect* **2024**, *9*, e202304042.

[42] Wang, X.; Huang, S. C.; Huang, T. X.; Su, H. S.; Zhong, J. H.; Zeng, Z. C.; Li, M. H. Tip-enhanced Raman spectroscopy for surfaces and interfaces. *Chem. Soc. Rev.* **2017**, *46*, 4020–4041.

[43] Yu, Q. Z.; Yao, Z. J.; Zhang, H. L.; Li, Z. B.; Chen, Z. X.; Xiong, H. Q. Transient stimulated Raman excited fluorescence spectroscopy. *J. Am. Chem. Soc.* **2023**, *145*, 7758–7762.

[44] Mestl, G. *In situ* Raman spectroscopy—a valuable tool to understand operating catalysts. *J. Mol. Catal. A: Chem.* **2000**, *158*, 45–65.

[45] Han, X. X.; Rodriguez, R. S.; Haynes, C. L.; Ozaki, Y.; Zhao, B. Surface-enhanced Raman spectroscopy. *Nat. Rev. Methods Primers* **2021**, *1*, 87.

[46] Hess, C. New advances in using Raman spectroscopy for the characterization of catalysts and catalytic reactions. *Chem. Soc. Rev.* **2021**, *50*, 3519–3564.

[47] Chen, M. P.; Liu, D.; Qiao, L. L.; Zhou, P. F.; Feng, J. X.; Ng, K. W.; Liu, Q. J.; Wang, S. P.; Pan, H. *In-situ/operando* Raman techniques for in-depth understanding on electrocatalysis. *Chem. Soc. Rev.* **2023**, *461*, 141939.

[48] Qiao, L. L.; Zhu, A. Q.; Liu, D.; An, K. Y.; Feng, J. X.; Liu, C. F.; Ng, K. W.; Pan, H. *In situ* reconstructed Cu/β-$Co(OH)_2$ tandem catalyst for enhanced nitrate electroreduction to ammonia in ampere-level. *Adv. Energy Mater.* **2024**, *14*, 2402805.

[49] Cao, D. X.; Sun, X.; Li, F.; Bak, S. M.; Ji, T. T.; Geiwitz, M.; Burch, K. S.; Du, Y. H.; Yang, G. C.; Zhu, H. L. Understanding electrochemical reaction mechanisms of sulfur in all-solid-state batteries through *operando* and theoretical studies. *Angew. Chem., Int. Ed.* **2023**, *62*, e202302363.

[50] Liu, Y. H.; Su, X. Z.; Ding, J.; Zhou, J.; Liu, Z.; Wei, X. J.; Yang, H. B.; Liu, B. Progress and challenges in structural, *in situ* and *operando* characterization of single-atom catalysts by X-ray based synchrotron radiation techniques. *Chem. Soc. Rev.* **2024**, *53*, 11850–11887.

[51] Ghosh, S.; Kouamé, N. A.; Ramos, L.; Remita, S.; Dazzi, A.; Deniset-Besseau, A.; Beaunier, P.; Goubard, F.; Aubert, P. H.; Remita, H. Conducting polymer nanostructures for photocatalysis under visible light. *Nat. Mater.* **2015**, *14*, 505–511.

[52] Hamoud, H. I.; Valtchev, V.; Daturi, M. Selective catalytic reduction of NO_x over Cu- and Fe-exchanged zeolites and their mechanical mixture. *Appl. Catal. B: Environ.* **2019**, *250*, 419–428.

[53] Li, J. L.; Yao, L. B.; Wu, D. Z.; King, J.; Chuang, S. S. C.; Liu, B.; Peng, Z. M. Electrocatalytic methane oxidation to ethanol on iron–nickel hydroxide nanosheets. *Appl. Catal. B: Environ.* **2022**, *316*, 121657.

[54] Huang, M. T.; Gu, Q.; Wu, Y. G.; Wei, Y. H.; Pei, Y. F.; Hu, T.; Lützenkirchen-Hecht, D.; Yuan, K.; Chen, Y. W. Linkage microenvironment and oxygen electroreduction reaction performance correlationship of iron phthalocyanine-based polymers. *Angew. Chem.* **2025**, *137*, e202501506.

[55] Chandrasekaran, S.; Wang, Q. P.; Liu, Q.; Wang, H. H.; Qiu, D. R.; Lu, H. D.; Liu, Y. P.; Bowen, C.; Huang, H. T. Dynamic regulation of ferroelectric polarization using external stimuli for efficient water splitting and beyond. *Chem. Soc. Rev.* **2025**, *54*, 2275–2343.

[56] Chen, Y. J.; Wang, X. Y.; Li, X. Y.; Miao, R. K.; Dong, J. C.; Zhao, Z. L.; Liu, C. H.; Huang, J. E.; Wu, J. H.; Chu, S. L. et al. Electrified synthesis of n-propanol using a dilute alloy catalyst. *Nat. Catal.* **2025**, *8*, 239–247.

[57] Liu, W. N.; An, L.; Li, P. F.; Fu, Y. J.; Zhang, X.; Qu, D.; Liu, Y. C.; Hu, P.; Wang, X. Y.; Jiang, N. et al. Regulating electronic density and interfacial electric field of high-entropy metallenes to enhance oxygen reduction reaction activity. *Chem Catal.* **2025**, *5*, 101357.

[58] Zhang, J.; Wang, M.; Gao, Z. R.; Qin, X. T.; Xu, Y.; Wang, Z. H.; Zhou, W.; Ma, D. Importance of species heterogeneity in supported metal catalysts. *J. Am. Chem. Soc.* **2022**, *144*, 5108–5115.

[59] Dai, Y.; Li, S. J.; Li, X.; Liu, K. H.; Guo, Y. N.; Li, H. X.; Jiang, B. Tandem active sites in Cu/Mo-WO_3 electrocatalysts for efficient electrocatalytic nitrate reduction to ammonia. *Adv. Funct. Mater.* **2025**, *35*, 2420282.

[60] Formanuik, A.; Ariciu, A. M.; Ortu, F.; Beekmeyer, R.; Kerridge, A.; Tuna, F.; McInnes, E. J. L.; Mills, D. P. Actinide covalency measured by pulsed electron paramagnetic resonance spectroscopy. *Nat. Chem.* **2017**, *9*, 578–583.

[61] Qin, Z. Y.; Wang, Z. C.; Kong, F.; Su, J.; Huang, Z. H.; Zhao, P. J.; Chen, S. Y.; Zhang, Q.; Shi, F. Z.; Du, J. F. *In situ* electron paramagnetic resonance spectroscopy using single nanodiamond

sensors. *Nat. Commun.* **2023**, *14*, 6278.
[62] Simpson, D. A.; Ryan, R. G.; Hall, L. T.; Panchenko, E.; Drew, S. C.; Petrou, S.; Donnelly, P. S.; Mulvaney, P.; Hollenberg, L. C. L. Electron paramagnetic resonance microscopy using spins in diamond under ambient conditions. *Nat. Commun.* **2017**, *8*, 458.
[63] Brückner, A. *In situ* electron paramagnetic resonance: A unique tool for analyzing structure–reactivity relationships in heterogeneous catalysis. *Chem. Soc. Rev.* **2010**, *39*, 4673–4684.
[64] Liu, X. W.; Zhao, L. J.; Shen, Y. Q.; Peng, W. H.; Mao, B. G.; Hou, J. H.; Wang, D.; Chen, X. C.; Dai, Y.; Zhang, C. J. et al. Hierarchical carbon-based electrocatalyst with functional separation properties for efficient pH universal nitrate reduction. *Adv. Mater.* **2025**, *37*, 2417623.
[65] Ma, S. Y.; Wang, K. X.; Rafique, M.; Han, J. C.; Fu, Q.; Jiang, S. D.; Wang, X. J.; Yao, T.; Xu, P.; Song, B. Reconstruction of ferromagnetic/paramagnetic cobalt-based electrocatalysts under gradient magnetic fields for enhanced oxygen evolution. *Angew. Chem.* **2024**, *136*, e202412821.
[66] Shao, Z. Y.; Zhu, Q.; Sun, Y.; Zhang, Y.; Jiang, Y. L.; Zhang, W. Q.; Zhang, W.; Huang, K. K.; Feng, S. H. Phase-reconfiguration-induced NiS/$NiFe_2O_4$ composite for performance-enhanced zinc-air batteries. *Adv. Mater.* **2022**, *34*, 2110172.
[67] Fan, K.; Xie, W. F.; Li, J. Z.; Sun, Y. N.; Xu, P. C.; Tang, Y.; Li, Z. H.; Shao, M. F. Active hydrogen boosts electrochemical nitrate reduction to ammonia. *Nat. Commun.* **2022**, *13*, 7958.
[68] Attar, F.; Yin, H.; Schumann, S. L.; Langley, J.; Cox, N.; Zeng, Z. Y.; Catchpole, K.; Karuturi, S.; Yin, Z. Y. Advanced electron paramagnetic resonance in chemical energy conversion: Current status and future potential. *Energy Environ. Sci.* **2024**, *17*, 3307–3328.
[69] Roessler, M. M.; Salvadori, E. Principles and applications of EPR spectroscopy in the chemical sciences. *Chem. Soc. Rev.* **2018**, *47*, 2534–2553.
[70] Zhang, H.; Chen, L.; Dong, F.; Lu, Z. W.; Lv, E. M.; Dong, X. L.; Li, H. X.; Yuan, Z. Y.; Peng, X. W.; Yang, S. H. et al. Dynamic transformation of active sites in energy and environmental catalysis. *Energy Environ. Sci.* **2024**, *17*, 6435–6481.
[71] Chao, H. Y.; Venkatraman, K.; Moniri, S.; Jiang, Y. J.; Tang, X.; Dai, S.; Gao, W. P.; Miao, J. W.; Chi, M. F. *In situ* and emerging transmission electron microscopy for catalysis research. *Chem. Rev.* **2023**, *123*, 8347–8394.
[72] Lewczuk, B.; Szyryńska, N. Field-emission scanning electron microscope as a tool for large-area and large-volume ultrastructural studies. *Animals* **2021**, *11*, 3390.
[73] Liu, Q.; Fu, Y. H.; Qin, Z. H.; Wang, Y.; Zhang, S. S.; Ran, M. M. Progress in the applications of atomic force microscope (AFM) for mineralogical research. *Micron* **2023**, *170*, 103460.
[74] Su, D. S.; Zhang, B. S.; Schlögl, R. Electron microscopy of solid catalysts—transforming from a challenge to a toolbox. *Chem. Rev.* **2015**, *115*, 2818–2882.
[75] Das, S.; Biswas, J.; Siddique, I. M. Mechanical characterization of materials using advanced microscopy techniques. *World J. Adv. Res. Rev.* **2024**, *21*, 274–283.
[76] Prajapati, A.; Hahn, C.; Weidinger, I. M.; Shi, Y. M.; Lee, Y.; Alexandrova, A. N.; Thompson, D.; Bare, S. R.; Chen, S.; Yan, S. et al. Best practices for *in-situ* and *operando* techniques within electrocatalytic systems. *Nat. Commun.* **2025**, *16*, 2593.
[77] Wang, G. W.; Ke, X. X.; Sui, M. L. Advanced TEM characterization for single-atom catalysts: From *ex-situ* towards *in-situ*. *Chem. Res. Chin. Univ.* **2022**, *38*, 1172–1184.
[78] Peng, L.; Peng, H. R.; Xu, L.; Wang, B. X.; Lan, K.; Zhao, T. C.; Che, R. C.; Li, W.; Zhao, D. Y. Anisotropic self-assembly of asymmetric mesoporous hemispheres with tunable pore structures at liquid–liquid interfaces. *J. Am. Chem. Soc.* **2022**, *144*, 15754–15763.
[79] Zhu, S. C.; Chen, G. W.; Yuan, X. H.; Cheng, Y.; Wan, M. H.; Xu, B. Y.; Wang, M. S.; Tang, H.; Hou, Y. L. Key for hexagonal diamond formation: Theoretical and experimental study. *J. Am. Chem. Soc.* **2025**, *147*, 2158–2167.
[80] Li, G. X.; Zhang, H.; Han, Y. Applications of transmission electron microscopy in phase engineering of nanomaterials. *Chem. Rev.* **2023**, *123*, 10728–10749.
[81] Liu, Y. J.; Xu, Y. B.; Tian, Y.; Guo, S.; Li, H. F.; Yuan, X. Y.; Zhao, Z. J.; Xu, B. C.; Wang, X. J.; Wang, P. et al. Frank partial dislocation pinning effect engineered IrNi alloy nanoparticles for water splitting. *ACS Catal.* **2025**, *15*, 3378–3390.
[82] Cheng, H. W.; Wang, S.; Chen, G. Y.; Liu, Z. W.; Caracciolo, D.; Madiou, M.; Shan, S. Y.; Zhang, J. C.; He, H. Y.; Chen, R. C. et al. Insights into heterogeneous catalysts under reaction conditions by *in situ*/*operando* electron microscopy. *Adv. Energy Mater.* **2022**, *12*, 2202097.
[83] De Alwis Goonatilleke, M.; Thomas, M. P.; Ullah, A.; Pham, R. H.; Guiton, B. S. Direct observation of sample dynamics in the gaseous environment: A perspective on current trends and future directions of *in situ* gas cell transmission electron microscopy. *J. Phys. Chem. C* **2023**, *127*, 18791–18808.
[84] Ramasundaram, S.; Jeevanandham, S.; Vijay, N.; Divya, S.; Jerome, P.; Oh, T. H. Unraveling the dynamic properties of new-age energy materials chemistry using advanced *in situ* transmission electron microscopy. *Molecules* **2024**, *29*, 4411.
[85] Tao, F.; Crozier, P. A. Atomic-scale observations of catalyst structures under reaction conditions and during catalysis. *Chem. Rev.* **2016**, *116*, 3487–3539.
[86] Tang, M.; Yuan, W. T.; Ou, Y.; Li, G. X.; You, R. Y.; Li, S. D.; Yang, H. S.; Zhang, Z.; Wang, Y. Recent progresses on structural reconstruction of nanosized metal catalysts via controlled-atmosphere transmission electron microscopy: A review. *ACS Catal.* **2020**, *10*, 14419–14450.
[87] Dai, J.; Sun, Y. F.; Liu, Z. W.; Zhang, Y. Y.; Duan, S. B.; Wang, R. M. Using *in situ* transmission electron microscopy to study strong metal–support interactions in heterogeneous catalysis. *Angew. Chem.* **2024**, *136*, e202409673.
[88] Tang, M.; Li, S. D.; Zhu, B. E.; You, R. Y.; Yu, L. J.; Ou, Y.; Yuan, W. T.; Xu, Q.; Yang, H. S.; Wales, D. J. et al. Oscillatory active state of a Pd nanocatalyst identified by *in situ* capture of the instantaneous structure–activity change at the atomic scale. *J. Am. Chem. Soc.* **2024**, *146*, 18341–18349.
[89] Davies, T. E.; Li, H.; Bessette, S.; Gauvin, R.; Patience, G. S.; Dummer, N. F. Experimental methods in chemical engineering: Scanning electron microscopy and X-ray ultra-microscopy—SEM and XuM. *Can. J. Chem. Eng.* **2022**, *100*, 3145–3159.
[90] Chee, S. W.; Lunkenbein, T.; Schlögl, R.; Roldán Cuenya, B. *Operando* electron microscopy of catalysts: The missing cornerstone in heterogeneous catalysis research. *Chem. Rev.* **2023**, *123*, 13374–13418.
[91] Lyu, Z. H.; Yao, L. H.; Chen, W. X.; Kalutantirige, F. C.; Chen, Q. Electron microscopy studies of soft nanomaterials. *Chem. Rev.* **2023**, *123*, 4051–4145.
[92] Liu, J. W.; You, F. T.; He, B. W.; Wu, Y. L.; Wang, D. D.; Zhou, W. Q.; Qian, C.; Yang, G. B.; Liu, G. F. Wang, H. et al. Directing the architecture of surface-clean Cu_2O for CO electroreduction. *J. Am. Chem. Soc.* **2022**, *144*, 12410–12420.
[93] Ma, X. Y.; Luo, W.; Yan, M. Y.; He, L.; Mai, L. Q. *In situ* characterization of electrochemical processes in one dimensional nanomaterials for energy storages devices. *Nano Energy* **2016**, *24*, 165–188.
[94] Qu, J. T.; Liu, X. Y. Recent advances on SEM-based *in situ* multiphysical characterization of nanomaterials. *Scanning* **2021**, *2021*, 4426254.
[95] Sagane, F.; Shimokawa, R.; Sano, H.; Sakaebe, H.; Iriyama, Y. *In-situ* scanning electron microscopy observations of Li plating and stripping reactions at the lithium phosphorus oxynitride glass electrolyte/Cu interface. *J. Power Sources* **2013**, *225*, 245–250.

[96] Cui, C.; Yang, H.; Zeng, C.; Gui, S. W.; Liang, J. N.; Xiao, P.; Wang, S. H.; Huang, G. X.; Hu, M. T.; Zhai, T. Y. et al. Unlocking the *in situ* Li plating dynamics and evolution mediated by diverse metallic substrates in all-solid-state batteries. *Sci. Adv.* **2022**, *8*, eadd2000.

[97] Sun, Z. F.; Pan, J. H.; Chen, W. W.; Chen, H. Y.; Zhou, S. H.; Wu, X. Y.; Wang, Y. S.; Kim, K.; Li, J.; Liu, H. D. et al. Electrochemical processes and reactions in rechargeable battery materials revealed via *in situ* transmission electron microscopy. *Adv. Energy Mater.* **2024**, *14*, 2303165.

[98] Stan, G.; King, S. W. Atomic force microscopy for nanoscale mechanical property characterization. *J. Vac. Sci. Technol. B* **2020**, *38*, 060801.

[99] Shen, Z. Z.; Zhang, Y. Z.; Zhou, C.; Wen, R.; Wan, L. J. Revealing the correlations between morphological evolution and surface reactivity of catalytic cathodes in lithium-oxygen batteries. *J. Am. Chem. Soc.* **2021**, *143*, 21604–21612.

[100] Wu, P. F.; Yang, Y. Q.; Xi, H. Y.; Si, Y.; Chu, Y. H.; Su, X. Z.; Yan, W. S.; You, T. T.; Gao, Y. K.; Wang, Y. et al. *Operando* spectroscopy observation of Mo clusters-$Ti_3C_2T_X$ catalyst/support interface's dynamic evolution in hydrogen evolution reaction. *Small* **2024**, *20*, 2306716.

[101] Li, T.; Wang, J. J.; Wang, F. L.; Zhang, L. S.; Jiang, Y. Y.; Arandiyan, H.; Li, H. The effect of surface wettability and coalescence dynamics in catalytic performance and catalyst preparation: A review. *ChemCatChem* **2019**, *11*, 1576–1586.

[102] Wang, C. P.; Wang, Z.; Mao, S. J.; Chen, Z. R.; Wang, Y. Coordination environment of active sites and their effect on catalytic performance of heterogeneous catalysts. *Chin. J. Catal.* **2022**, *43*, 928–955.

[103] Isahak, W. N. R. W.; Al-Amiery, A. Catalysts driving efficiency and innovation in thermal reactions: A comprehensive review. *Green Technol. Sustain.* **2024**, *2*, 100078.

[104] Lakhani, P.; Bhanderi, D.; Modi, C. K. Nanocatalysis: Recent progress, mechanistic insights, and diverse applications. *J. Nanopart. Res.* **2024**, *26*, 148.

[105] Rawat, K.; Sharma, N.; Singh, V. K. X-ray fluorescence and comparison with other analytical methods (AAS, ICP-AES, LA-ICP-MS, IC, LIBS, SEM-EDS, and XRD). In *X-Ray Fluorescence in Biological Sciences: Principles, Instrumentation, and Applications*. Singh, V. K.; Kawai, J.; Tripathi, D. K., Eds.; Wiley: Hoboken, **2022**; pp 1–20.

[106] Tao, F. Development of new methods of studying catalyst and materials surfaces with ambient pressure photoelectron spectroscopy. *Acc. Chem. Res.* **2025**, *58*, 11–23.

[107] Ischenko, A. A.; Weber, P. M.; Miller, R. J. D. Capturing chemistry in action with electrons: Realization of atomically resolved reaction dynamics. *Chem. Rev.* **2017**, *117*, 11066–11124.

[108] Bordiga, S.; Groppo, E.; Agostini, G.; van Bokhoven, J. A.; Lamberti, C. Reactivity of surface species in heterogeneous catalysts probed by *in situ* X-ray absorption techniques. *Chem. Rev.* **2013**, *113*, 1736–1850.

[109] Delgass, W. N.; Wolf, E. E. Catalytic surfaces and catalyst characterization methods. In *Chemical Reaction and Reactor Engineering*. Carberry, J. J., Ed.; CRC Press: Boca Raton, **1986**; pp 151–238.

[110] Weldon, M. K.; Friend, C. M. Probing surface reaction mechanisms using chemical and vibrational methods: Alkyl oxidation and reactivity of alcohols on transitions metal surfaces. *Chem. Rev.* **1996**, *96*, 1391–1412.

[111] Qin, R. X.; Liu, K. L.; Wu, Q. Y.; Zheng, N. F. Surface coordination chemistry of atomically dispersed metal catalysts. *Chem. Rev.* **2020**, *120*, 11810–11899.

[112] Gao, L. K.; Cui, X.; Sewell, C. D.; Li, J.; Lin, Z. Q. Recent advances in activating surface reconstruction for the high-efficiency oxygen evolution reaction. *Chem. Soc. Rev.* **2021**, *50*, 8428–8469.

[113] Zhao, H. L.; Liu, P. F.; Cheng, X. T.; Fan, C.; Liu, J.; Kan, D. X.; Wang, Y. Q. A Cu-Cu_2O/Ni_2P heterostructure for efficient tandem catalysis of electrosynthesis of ammonia from nitrate reduction reaction in neutral medium. *Adv. Funct. Mater.* **2025**, *35*, 2425459.

[114] Wang, R. F.; Liu, Y. C.; Kong, Y. F.; Xie, P.; Zhao, S. L. Hierarchically structured SnO/$NiCo_2O_4$/CC catalysts with stability and superior faradaic efficiency for electrocatalytic CO_2 reduction to formic acid. *Chem. Eng. J.* **2023**, *469*, 144049.

[115] He, M.; Huang, L. J.; Zhao, B. S.; Chen, B. B.; Hu, B. Advanced functional materials in solid phase extraction for ICP-MS determination of trace elements and their species—a review. *Anal. Chim. Acta* **2017**, *973*, 1–24.

[116] Yan, K.; Lee, S. W.; Yap, K. M. K.; Mule, A. S.; Hannagan, R. T.; Matthews, J. E.; Kamat, G. A.; Lee, D. U.; Stevens, M. B.; Nielander, A. C. et al. On-line inductively coupled plasma mass spectrometry reveals material degradation dynamics of Au and Cu catalysts during electrochemical CO_2 reduction. *J. Am. Chem. Soc.* **2025**, *147*, 4079–4088.

[117] van der Merwe, M.; Garcia-Diez, R.; Lahn, L.; Wibowo, R. E.; Frisch, J.; Gorgoi, M.; Yang, W. L.; Ueda, S.; Wilks, R. G.; Kasian, O. et al. The chemical and electronic properties of stability-enhanced, mixed Ir-TiO_x oxygen evolution reaction catalysts. *ACS Catal.* **2023**, *13*, 15427–15438.

[118] Bulavchenko, O. A.; Vinokurov, Z. S. *In situ* X-ray diffraction as a basic tool to study oxide and metal oxide catalysts. *Catalysts* **2023**, *13*, 1421.

[119] Bunaciu, A. A.; Udriştioiu, E. G.; Aboul-Enein, H. Y. X-ray diffraction: Instrumentation and applications. *Crit. Rev. Anal. Chem.* **2015**, *45*, 289–299.

[120] Li, J.; Sun, J. L. Application of X-ray diffraction and electron crystallography for solving complex structure problems. *Acc. Chem. Res.* **2017**, *50*, 2737–2745.

[121] Li, G. N.; Priyadarsini, A.; Xie, Z. H.; Kang, S.; Liu, Y. Z.; Chen, X. B.; Kattel, S.; Chen, J. G. Achieving higher activity of acidic oxygen evolution reaction using an atomically thin layer of IrO_x over Co_3O_4. *J. Am. Chem. Soc.* **2025**, *147*, 7008–7016.

[122] Yi, W. L.; Hou, C. S.; Li, R. Y.; Wan, Y. J.; Zhang, X.; Ma, B.; Hu, W. C.; Han, S. H.; Qin, M. L.; Sun, L. M. et al. Designer electron-reservoir single-atom electrocatalyst for efficient carbon dioxide reduction. *Chem. Eng. J.* **2025**, *507*, 160387.

[123] Liu, H.; Huang, M. Y.; Tao, W. L.; Han, L. L.; Zhang, J. Q.; Zhao, Q. S. A palladium catalyst supported on boron-doped porous carbon for efficient dehydrogenation of formic acid. *Nanomaterials* **2024**, *14*, 549.

[124] Li, Y. O.; Wang, K.; Wang, Z. J.; Wang, X. M.; Chu, X.; Zhang, R.; Song, S. Y.; Zhang, H. J.; Wang, X. Ultra-fast synthesis of composite oxide-supported transition metal alloy as an advanced catalyst for ammonia decomposition. *Adv. Energy Mater.* **2025**, *15*, 2405296.

[125] Zhao, J. H.; Wang, Y. F.; Liu, H.; Zhang, R.; Jia, W. L.; Zhang, J. H.; Sun, Y.; Peng, L. C. Understanding the role of dual zinc and indium vacancies in $ZnIn_2S_4$ for the visible-light-driven photocatalytic air-oxidation of 5-hydroxymethylfurfural. *ACS Catal.* **2025**, *15*, 3464–3474.

[126] Yang, P. C.; Gao, D. L.; Yang, Y. J.; Jia, Z. Y.; Li, Y. Q.; Xia, J.; Yi, D.; Wang, X.; Yang, Y. A. Enhancing d–p orbital coupling by Hf doping to construct a stable $LiMn_2O_4$ cathode for lithium-ion batteries. *Nano Energy* **2024**, *125*, 109570.

[127] Bon, V.; Brunner, E.; Pöppl, A.; Kaskel, S. Unraveling structure and dynamics in porous frameworks via advanced *in situ* characterization techniques. *Adv. Funct. Mater.* **2020**, *30*, 1907847.

[128] Guo, W. H.; Zhang, K. X.; Liang, Z. B.; Zou, R. Q.; Xu, Q. Electrochemical nitrogen fixation and utilization: Theories, advanced catalyst materials and system design. *Chem. Soc. Rev.* **2019**, *48*, 5658–5716.

[129] Chen, J.; Zhang, Y. T.; Zhang, Z. H.; Hou, D. Y.; Bai, F. N.; Han, Y.; Zhang, C. X.; Zhang, Y. J.; Hu, J. Metal–support interactions for heterogeneous catalysis: Mechanisms, characterization techniques and applications. *J. Mater. Chem. A* **2023**, *11*, 8540–8572.

[130] Clayson, I. G.; Hewitt, D.; Hutereau, M.; Pope, T.; Slater, B. High throughput methods in the synthesis, characterization, and optimization of porous materials. *Adv. Mater.* **2020**, *32*, 2002780.

[131] Hołyńska, M.; Tighe, A.; Semprimoschnig, C. Coatings and thin films for spacecraft thermo-optical and related functional applications. *Adv. Mater. Interfaces* **2018**, *5*, 1701644.

[132] Morgan, D.; Pilania, G.; Couet, A.; Uberuaga, B. P.; Sun, C.; Li, J. Machine learning in nuclear materials research. *Curr. Opin. Solid State Mater. Sci.* **2022**, *26*, 100975.

[133] Dou, B. Z.; Zhu, Z. L.; Merkurjev, E.; Ke, L.; Chen, L.; Jiang, J.; Zhu, Y. Y.; Liu, J.; Zhang, B. G.; Wei, G. W. Machine learning methods for small data challenges in molecular science. *Chem. Rev.* **2023**, *123*, 8736–8780.

[134] Kumar, V.; Nisika; Kumar, M. Temporal-spatial-energy resolved advance multidimensional techniques to probe photovoltaic materials from atomistic viewpoint for next-generation energy solutions. *Energy Environ. Sci.* **2021**, *14*, 4760–4802.

[135] Carter, S.; Fisher, A. S.; Hinds, M. W.; Lancaster, S. Atomic spectrometry update. Industrial analysis: Metals, chemicals and advanced materials. *J. Anal. At. Spectrom.* **2012**, *27*, 2003–2053.

[136] Sen-Britain, S. T.; Keilbart, N. D.; Kweon, K. E.; Pham, T. A.; Orme, C. A.; Wood, B. C.; Nelson, A. J. *Characterization of Surface Oxide Chemistry of New and Recycled Ti–Al Alloy Powders Used in Laser Powder Bed Fusion Additive Manufacturing*; Lawrence Livermore National Laboratory: Livermore, **2020**; pp 157–161.

[137] Wytrwal-Sarna, M.; Sekuła-Stryjewska, M.; Pomorska, A.; Ocłoń, E.; Gajos, K.; Sarna, M.; Zuba-Surma, E.; Bernasik, A.; Szczubiałka, K. The effect of the topmost layer and the type of bone morphogenetic protein-2 immobilization on the mesenchymal stem cell response. *Int. J. Mol. Sci.* **2022**, *23*, 9287.

[138] Sahu, M.; Gupta, R.; Ambasta, R. K.; Kumar, P. Artificial intelligence and machine learning in precision medicine: A paradigm shift in big data analysis. *Prog. Mol. Biol. Transl. Sci.* **2022**, *190*, 57–100.

[139] Kartashov, O. O.; Chernov, A. V.; Polyanichenko, D. S.; Butakova, M. A. XAS data preprocessing of nanocatalysts for machine learning applications. *Materials* **2021**, *14*, 7884.

[140] Papia, E. M.; Kondi, A.; Constantoudis, V. Machine learning applications in SEM-based pore analysis: A review. *Microporous Mesoporous Mater.* **2025**, *394*, 113675.

[141] Yao, L. H.; Ou, Z. H.; Luo, B. B.; Xu, C.; Chen, Q. Machine learning to reveal nanoparticle dynamics from liquid-phase TEM videos. *ACS Cent. Sci.* **2020**, *6*, 1421–1430.